Journal of Environmental Management 347 (2023) 119071

Contents lists available at ScienceDirect

Journal of Environmental Management

journal homepage: www.elsevier.com/locate/jenvman

Research article

Appraisal of agroforestry biomass wastes for hydrogen production by an integrated process of fast pyrolysis and in line steam reforming

Aitor Arregi [a], Laura Santamaria [b], Gartzen Lopez [b,c,*], Martin Olazar [b], Javier Bilbao [b], Maite Artetxe [b], Maider Amutio [b]

[a] Department of Chemical and Environmental Engineering, University of the Basque Country UPV/EHU, Nieves Cano 12, Vitoria-Gasteiz, 01006, Spain
[b] Department of Chemical Engineering, University of the Basque Country UPV/EHU, P.O. Box 644, E48080, Bilbao, Spain
[c] IKERBASQUE, Basque Foundation for Science, Bilbao, Spain

ARTICLE INFO

Handling Editor: Prof Raf Dewil

Keywords:
Pine wood
Citrus waste
Rice husk
Pyrolysis
Reforming
Hydrogen

ABSTRACT

The pyrolysis and in line steam reforming of different types of representative agroforestry biomass wastes (pine wood, citrus wastes and rice husk) was performed in a two-reactor system made up of a conical spouted bed and a fluidized bed. The pyrolysis step was carried out at 500 °C, and the steam reforming at 600 °C with a space time of 20 $g_{catalyst}$ min $g^{-1}_{volatiles}$ and a steam/biomass ratio (S/B) of 4. A study was conducted on the effect that the pyrolysis volatiles composition obtained with several biomasses has on the reforming conversion, product yields and H_2 production. The different composition of the pyrolysis volatiles obtained with the three biomasses studied led to differences in the initial activity and, especially, in the catalyst deactivation rate. Initial conversions higher than 99% were obtained in all cases and the H_2 production obtained varied in the 6.7–11.2 wt% range, depending on the feedstock used. The stability of the catalysts decreased depending on the feedstock as follows: pine wood ≫ citrus waste > rice husk. A detailed assessment of the mechanisms of catalyst deactivation revealed that coke deposition is the main cause of catalyst decay in all the runs. However, the volatile composition derived from the pyrolysis of citrus waste and rice husk involved the formation of an encapsulating coke, which severely blocked the catalyst pores, leading to catalyst deactivation during the first minutes of reaction.

1. Introduction

The amount of agro-industrial wastes has been increased in the last years due to the high demand of related feedstocks for food production (Freitas et al., 2021). Most of these wastes are incinerated or disposed in landfills and, in some cases, used to produce animal feed or recover energy (Cristóbal et al., 2018; Stone et al., 2019). Although a responsible production of food must involve minimization of wastes, the inedible parts of food wastes must be treated. These wastes can be used as feedstock in biorefineries to produce valuable products and chemicals (Cormos, 2023). Recently, new technologies for food waste valorization have been developed in order to step forward in the biorefinery concept (Caldeira et al., 2020; De Laurentiis et al., 2018; Kurniawan et al., 2023). Moreover, their valorization can contribute to the production of high value-added products and chemicals by sustainable pathways using renewable sources, and therefore help to decrease the current dependency on fossil resources.

Among the wastes from food production, citrus peel waste is an interesting alternative biomass source and has been recently considered as a promising feedstock for the production of fuels and chemicals (Caldeira et al., 2020; Jeong et al., 2021; Ong et al., 2018). Thus, thanks to their high availability, since citrus fruits are the most cultivated fruits over the world, their production has reached around 124 million tons per year (Patsalou et al., 2020). Furthermore, most of this amount is used for food processing and, especially, for juice production, which leads to close to 54 million tons per year of citrus wastes, mainly composed of citrus peel waste (Teigiserova et al., 2021). Citrus wastes have a high organic and water content and a low pH, and therefore the European legislation does not allow their disposal in landfills (Santiago et al., 2020). Biological routes for orange waste valorization have proven to be viable for the production of different chemicals (Jeong et al., 2021), but the high concentration of essential oils, such as limonene, is the main problem for the valorization via this route due to the anti-microbial properties of these oils (Zema et al., 2018). Nevertheless, thermochemical routes have also proven to be highly relevant, especially those involving gasification (Galvagno et al., 2019; Vargas et al.,

* Corresponding author. Department of Chemical Engineering, University of the Basque Country UPV/EHU, P.O. Box 644, E48080, Bilbao, Spain.
E-mail address: gartzen.lopez@ehu.es (G. Lopez).

https://doi.org/10.1016/j.jenvman.2023.119071
Received 9 March 2023; Received in revised form 7 June 2023; Accepted 30 August 2023
Available online 4 October 2023

2015) and pyrolysis processes (Alvarez et al., 2018; Kim et al., 2016; Lam et al., 2018).

Rice husk is one of the most available agricultural residues, as it accounts for approximately 134 million tons per year worldwide (Quispe et al., 2017). It is mainly composed of hemicellulose, cellulose and lignin, and therefore is suitable for the production of fuels and chemicals (Moogi et al., 2021). Moreover, thermochemical processes, such as direct combustion, have been the most used ones in order to recover energy (Quispe et al., 2017). Recently, fast pyrolysis has gained attention for bio-oil production from rice husk due to its efficiency (Alvarez et al., 2014; Tian et al., 2021) and flexibility involving operating conditions, apart from the possibility of jointly feeding other types of biomasses (Bushra and Remya, 2020). The bio-oils produced by pyrolysis of citrus wastes or rice husk are not suitable for direct use due to their high content of water, oxygen and ash, and therefore low energy density (Chang, 2020). In fact, the deterioration of rice husk bio-oil properties, as well as the tendency of certain compounds (especially, alcohols, furans and hydrocarbons) to accumulate on the bottom layer has been reported (Cai et al., 2019). Attempts have been made to improve this bio-oil through another in-line step, usually a catalytic pyrolysis step, but a rather limited success has been attained.

In this scenario, the pyrolysis and in line upgrading by catalytic steam reforming has been proposed as an alternative pathway to avoid these problems related to bio-oil storage, given that the volatiles obtained in the pyrolysis step are directly driven into the reforming step (Arregi et al., 2018a; Lopez et al., 2022; Santamaria et al., 2021). This original route has been recently developed using several reactor configurations, with the most common one being two fixed beds connected in series (Cao et al., 2017; Waheed et al., 2016; Xiao et al., 2013) operating in batch regime. However, there is hardly any study dealing with reaction units operating in continuous regime, such as a battery of a fluidized bed with a fixed bed (Wang et al., 2013; Xiao et al., 2011) or a spouted bed with a fluidized or fixed bed (Fernandez et al., 2021, 2022a). Apart from avoiding the problems related to bio-oil storage, the main advantages of this strategy are as follows (Arregi et al., 2018a): i) temperature can be independently optimized in each step; ii) the direct contact between the feedstock impurities and the catalyst is avoided; iii) Ni sintering can be avoided due to the relatively low temperature used, and; iv) full conversion can be achieved without tar production. In addition, this process allows obtaining a H_2-rich gas product. It should be highlighted that H_2 is one of the promising sustainable energy carriers in the future and currently a widely used compound in industry, mainly for ammonia production and oil refining (Khademi and Lotfi-Varnoosfaderani, 2021). Therefore, the use of different types of biomasses may be an interesting alternative for H_2 production, as this would allow reducing the dependency on fossil fuels.

This study deals with the upgrading of the pyrolysis volatile components (bio-oil and gases) from different biomasses (pine wood, citrus wastes and rice husk) in a novel integrated process made up of continuous pyrolysis and in line catalytic steam reforming. A Ni commercial reforming catalyst has been used, which has shown a good performance in previous studies dealing with biomass pyrolysis-reforming carried out by our research group (Arregi et al., 2016, 2018b, 2018c, 2018d). Apart from biomass, this technology performs well in the treatment of different types of wastes, such as plastics (Barbarias et al., 2016, 2018) or even biomass/plastic mixtures (Arregi et al., 2017). Nevertheless, given the availability of different types of biomasses, studies involving their joint treatment are essential in order to assess process flexibility. Therefore, this study deals with the effect that feedstock nature has on the conversion of the pyrolysis volatile stream, product yields and gas composition. Moreover, catalyst deactivation has also been studied in depth, analyzing the catalyst performance with time on stream and characterizing the deactivated catalysts by N_2 adsorption-desorption, X-ray diffraction (XRD), ultimate analysis, temperature programmed oxidation (TPO) and transmission electron microscopy (TEM) images. The results obtained in this study will allow establishing the main mechanisms of catalyst decay and provide further knowledge about the role played by bio-oil composition in the deactivation of the reforming catalyst.

2. Experimental

2.1. Feedstock properties and catalyst characterization

Several feedstocks (pine wood waste, citrus wastes and rice husk) were tested in the pyrolysis-reforming process. Considering the different characteristics of the biomasses, each feedstock was pretreated in a different way prior to its valorization in order to ease continuous feeding. Pine wood waste was directly ground and sieved to obtain pine wood sawdust with a particle size ranging between 1 and 2 mm (Arregi et al., 2016). Citrus wastes were first dried for 24 h at 60 °C to a moisture content of 1.5 wt%, and the pretreated wastes were then ground and sieved to remove particles with size lower than 1 mm (Alvarez et al., 2018). Rice husk supplied by Brillante brand (Ebro Foods S.A) was ground and sieved to a particle size in the 0.63–1 mm range. Although the conical spouted bed reactor (CSBR) allows treating a very wide range of particle sizes (Alvarez et al., 2014), the range selected is the most suitable for the feeder available in the laboratory unit.

Table 1 shows the main features of the feedstocks, which were measured in a LECO CHNS-932 elemental analyzer (ultimate analysis) and in a TGA Q5000IR thermogravimetric analyzer (proximate analysis). Moreover, the analysis of the data obtained by TGA allows determining the main chemical constituents of the different biomasses, i.e., hemicelluloses, cellulose, lignin and pectin, with the latter being only contained in citrus wastes. Besides, an isoperibolic bomb calorimeter (Parr 1356) was used to measure the higher heating value (HHV). The chemical composition of the ash determined by X-ray fluorescence (model AXIOS, PANalytical) is set out in Table 2.

As observed in Table 1, pine wood sawdust has higher C content compared to the other feedstocks (49.1 wt%, 42.7 wt% and 42.0 wt% for pine waste, citrus waste and rice husk, respectively). Besides, the lower amount of fixed carbon and, especially, that of ashes contained in the pine wood makes this biomass a suitable feedstock for valorization and H_2 production through the pyrolysis-reforming process. Conversely, the rice husk biomass has a high ash content (12.9 wt%), which is mainly composed of silica (Table 2). This high ash content may negatively affect the overall H_2 production in the process, since it means a lower amount of volatiles to be fed into the reforming reactor. Moreover, it is to note that considerable differences have been observed in the concentrations

Table 1
Feedstock characterization.

Feedstock	Pine wood	Citrus waste	Rice husk
Ultimate analysis (wt%)[a]			
Carbon	49.08	42.7	42.0
Hydrogen	6.03	6.4	5.4
Nitrogen	0.04	1.0	0.4
Oxygen[b]	44.35	47.6	39.3
Proximate analysis (wt%)[c]			
Volatile matter	73.4	74.1	70.5
Fixed carbon	16.7	23.6	16.6
Ash	0.5	2.3	12.9
Moisture	9.4	1.5	1.1
Macromolecular composition (wt%)[d]			
Cellulose	51.0	17.5	46.4
Hemicellulose	23.0	17.0	21.7
Lignin	26.0	29.4	31.9
Pectin	–	36.1	–
HHV (MJ kg^{-1})	19.8	19.4	16.8

[a] on a dry basis.
[b] by difference.
[c] on an air-dried basis.
[d] on an ash free basis.

Table 2
Chemical analysis of the ash (wt%).

Feedstock	Pine wood	Citrus waste	Rice husk
SiO_2	8.84	0.29	98.02
Al_2O_3	2.38	0.33	0.52
Fe_2O_3	2.30	0.09	0.11
MnO	2.46	–	0.01
MgO	10.44	4.78	0.11
CaO	32.34	29.47	0.23
Na_2O	1.93	1.98	0.10
K_2O	11.30	30.9	0.38
TiO_2	0.11	0.02	0.02
P_2O_5	2.55	8.34	0.08
SO_3	3.59	3.46	–

of the main components of each biomass. Thus, pinewood and rice husk are lignocellulosic biomasses, with a cellulose content of around 46.4 and 51.0 wt%, a hemicellulose content between 21.7 and 23.0 wt% and a lignin one in the range from 26.0 to 31.9 wt%. However, the citrus waste is made up of 36.1 wt% pectin, 17.0 wt% hemicellulose and 17.5 wt% cellulose, with the remaining 29.4 wt% being lignin, proteins and soluble sugars, as well as certain fats (Alvarez et al., 2018). Accordingly, the product distribution in the pyrolysis stream depends on the composition of the biomass.

A commercial catalyst from Clariant's ReforMax series was used (Reformax® 330 LDP). This catalyst is a calcium-promoted nickel-based one, which is highly active for a variety of reforming processes and feed conditions. This catalyst was crushed and sieved to a particle size in the 0.4–0.8 mm range, for the purpose of obtaining a good fluidization regime in the reforming step. In previous studies, the catalyst was characterized in detail by N_2 adsorption-desorption (*Micromeritics ASAP 2010*) and temperature programmed reduction (TPR) (*Micromeritics AutoChem 2920*). The catalyst has a low BET surface area (19 $m^2\ g^{-1}$) and pore volume (0.04 $cm^3\ g^{-1}$). The reduction temperature of the catalyst was established at 710 °C following the results obtained in the TPR analysis, ensuring full reduction of NiO and $NiAl_2O_4$ spinel phases. A 10 vol% H_2 in N_2 stream was used for the reduction of the catalyst during 4 h. More details about the characterization and properties of the catalyst can be found elsewhere (Arregi et al., 2017; Santamaria et al., 2020a).

The textural properties of the deactivated catalysts were determined by N_2 adsorption-desorption (*Micromeritics ASAP 2010*), following the same procedure as the one conducted in the fresh catalyst. Moreover, the amount of sulfur on the spent samples was quantified using a *LECO CHNS-932* elemental analyzer.

X-ray powder diffraction (XRD) patterns of both fresh (reduced) and deactivated catalysts were obtained in a *Bruker D8 Advance* diffractrometer, and the Ni crystallite size was estimated based on the Debye Scherrer equation.

The deactivated catalysts were also characterized by temperature programmed oxidation (TPO) analysis in a *TA Instruments TGA Q5000IR*. Firstly, the sample was thermally treated with a N_2 stream (50 mL min^{-1}) at 200 °C for 20 min in order to remove the water contained in the sample. Temperature was then reduced to 100 °C, and the N_2 flow was replaced with air (50 mL min^{-1}), keeping these condition for 5 min until the signal was stabilized. Subsequently, the sample was oxidized with an air flow of 50 mL min^{-1} from 100 °C to 800 °C and kept at that temperature for another 30 until full coke combustion. The same procedure was followed for the fresh reduced catalyst in order to account for the mass gain derived from the metal oxidation. In addition, transmission electron microscopy (TEM) images were obtained in a *Philips CM200* apparatus in order to draw information about the location and nature of the coke.

2.2. Reaction equipment and experimental conditions

The general scheme of the pilot plant used in the pyrolysis-reforming process is shown in Fig. 1. It has been developed based on previous studies by the research group, in which the unit performed well in the pyrolysis and in line steam reforming of biomass, plastics, and biomass/plastic mixtures (Arregi et al., 2017, 2018b; Barbarias et al., 2016). The bench scale plant consists of the following components: feeding devices for solid, gas and water streams, reaction units, the product separation system and devices for the analysis of the outlet gaseous stream.

The solid feeding dispenser consists of a dosage cylinder provided with a piston and a vibrator. The different feeds (pine wood, citrus waste or rice husk) are loaded into the dispenser through an inlet located at the top of the feeding system. The piston pushes the solid towards the top of the feeding dispenser, where it falls into the reactor through a cooled tube. Different gases (N_2 and H_2) can also be fed into the lower part of the pyrolysis reactor, i.e., N_2 as an inert gas, and H_2 for the reduction of the catalyst prior to use in the reforming step. Water is fed into the system by means of a *Gilson 307* positive displacement pump and vaporized by an evaporator prior to entering the reactor.

The main elements of the reaction system are the conical spouted bed reactor (CSBR) for the pyrolysis of the biomasses and the fluidized bed reactor (FBR) for the in line steam reforming of the volatiles produced in the pyrolysis reactor. The pyrolysis reactor is a CSBR, which has a lower conical section and an upper cylindrical one. The specific dimensions of the CSBR, which can be found elsewhere (Arregi et al., 2016), ensure the stability of the bed with a great versatility involving operating conditions. This versatility allows working with a wide range of gas flow rates. Thus, high gas flow rates lead to high particle velocities, and therefore high turbulence, avoiding the segregation in the bed. Moreover, the char formed is continuously removed from the pyrolysis reactor by means of a lateral outlet pipe to avoid its accumulation in the bed. The operating conditions used in the runs were established based on the prior knowledge by the research group (Amutio et al., 2012; Arregi et al., 2016, 2018b), and are as follows: pyrolysis temperature, 500 °C (the optimum one to maximize bio-oil production); biomass flow rate, 0.75 g min^{-1}; water flow rate, 3 mL min^{-1}; sand mass, 30 g; and sand particle size, 0.30–0.35 mm. Furthermore, the FBR is a cylindrical reforming reactor made up of stainless steel, with an internal diameter of 38.1 mm and a length of 440 mm. Likewise, based on previous parametric and hydrodynamic studies, the following operating conditions were selected: reforming temperature, 600 °C; space time, 20 $g_{catalyst}\ min\ g^{-1}_{volatiles}$; steam/biomass ratio (S/B), 4; catalyst particle size, 0.40–0.80 mm; and sand particle size, 0.30–0.35 mm.

The product separation system consists of a cyclone and a filter. The cyclone is placed between the CSBR and FBR in order to remove the char and sand particles and the filter is located after the FBR in order to remove the fine catalyst particles formed by attrition and entrained from the bed. Furthermore, the unit is provided with a pressure gauge, which detects increases in pressure drop caused by filter clogging, and therefore the need for its replacement. Both reactors, the cyclone and the filter are located inside an oven in which a temperature of 300 °C is maintained. This oven avoids the condensation of heavy compounds upstream and downstream the FBR, which is essential to avoid the condensation of volatile products (especially in the outlet stream) prior to the chromatographic analysis. In addition, the system for gas-liquid separation consists of a condenser made up of double shell tube and a coalescence filter to retain the micro-droplets (fog) in the gaseous stream.

2.3. Product analysis

The products obtained in the pyrolysis of different biomasses were analyzed prior to reforming. The gases and liquid products were analyzed by on-line chromatographic techniques. On the one hand, in order to quantify the products, the sample was first diluted with an inert

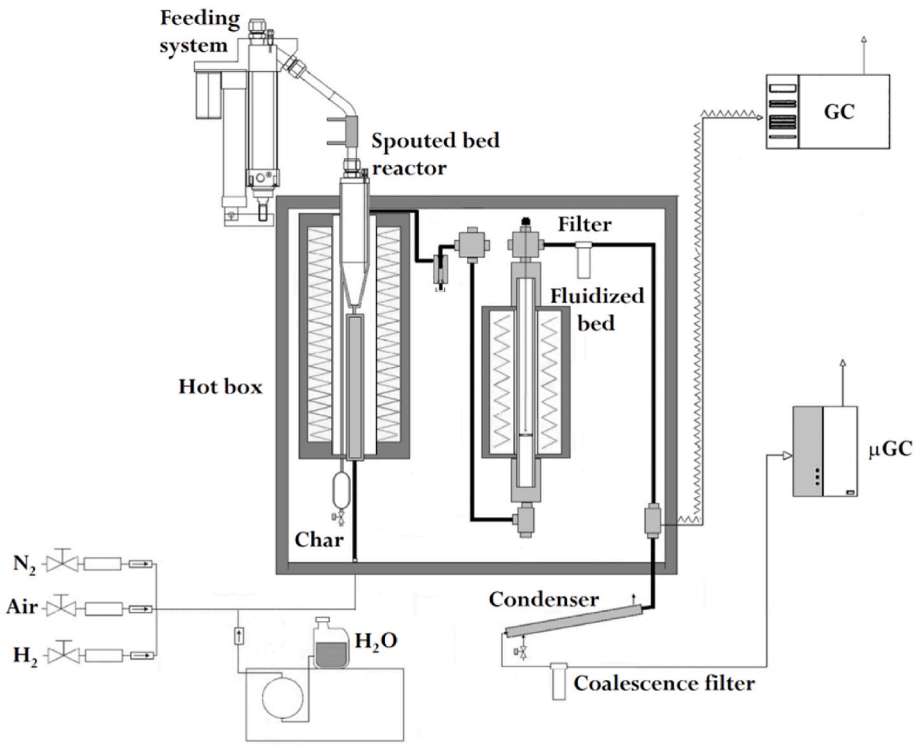

Fig. 1. Continuous bench scale plant for biomass pyrolysis and in line steam reforming.

gas, then mixed with 0.05 mL min^{-1} of an internal standard (cyclohexane, Panreac, 99.5%) and, finally, injected into a gas chromatograph *GC Varian 3900* by means of a line thermostated at 280 °C. This GC is equipped with a sampling valve (6-port valves), an injector (split/splitless type), a HP-Pona column and a flame ionization detector (FID). Besides, FID response factors determined in previous studies were used in the GC for the quantification of the bio-oil compounds, which correspond to different bio-oil families, such as phenols, ketones, aldehydes and saccharides, among others (Alvarez et al., 2018). Moreover, the identification of these compounds was carried out by means of a gas chromatograph-mass spectrometer *(GC-MS Shimadzu QP-2010S)* by analyzing the collected liquid using a similar column as in the GC. A detailed description of all analytical devices is provided in the Supplementary information. Furthermore, a gas micro-chromatograph *(GC Varian 4900)* was used for the analysis of the permanent gases (H_2, CH_4, CO, CO_2 and C_2–C_3), which was equipped with three channels and three analytical modules, as well as the injector, column and detector. Finally, the mass balance was closed by weighing the char collected by the lateral outlet.

The condensable volatile components and permanent gases obtained in the pyrolysis-reforming runs were analyzed in-line by a gas chromatograph *(GC Varian 3900)* and gas micro-chromatograph *(GC Varian 4900)*, respectively, described above. Samples of the volatile stream were extracted prior to condensing the reforming product stream, whereas the sampling point of the permanent gases was located after the condensation system. Moreover, the runs have been repeated at least 3 times under the same experimental conditions in order to ensure reproducibility of the results. Standard deviations of the results were determined from these runs.

2.4. Reaction indices

The main reaction indices for the monitoring of the process are as follows: conversion, the yields of C containing products and H_2, the production of H_2 and gaseous stream, and the amount of steam reacted.

- *Conversion (X, %):* It is defined as the C moles recovered in the gaseous product stream (C_{gas}) over those fed into the reforming step ($C_{volatiles}$).

$$X\,(\%) = \frac{C_{gas}}{C_{volatiles}} \cdot 100 \tag{1}$$

- *C containing product yields (Y_i, %):* They are defined as the molar flow rate of C moles contained in each product i (F_i) over the molar flow rate of C in the volatile stream entering the reforming reactor ($F_{volatiles}$).

$$Y_i(\%) = \frac{F_i}{F_{volatiles}} \cdot 100 \tag{2}$$

- *H_2 yield (Y_{H2}, %):* It is defined as the percentage of the maximum allowed by stoichiometry, with F_{H2} and F^0_{H2} being the H_2 molar flow rate obtained in the run and that calculated by stoichiometry, respectively:

$$Y_{H_2}(\%) = \frac{F_{H_2}}{F_{H_2}{}^0} \cdot 100 \tag{3}$$

- *H_2 production (P_{H2}, wt%):* It is defined as the ratio between the mass flow rate of H_2 produced (m_{H2}) and the mass flow rate of biomass fed into the pyrolysis reactor (m_0).

$$P_{H_2}(\mathrm{wt}\%) = \frac{m_{H_2}}{m_0} \cdot 100 \tag{4}$$

- *Gas production (P_{gas}, wt%):* It is defined as the ratio between the mass flow rate of gas produced (m_{gas}) and the mass flow rate of biomass fed into the pyrolysis reactor (m_0).

$$P_{gas}(\mathrm{wt}\%) = \frac{m_{gas}}{m_0} \cdot 100 \tag{5}$$

- *Reacted steam (R_{steam}, wt%):* It is the amount of steam reacted in the reforming reaction by mass unit of the biomass fed into the process.

$$R_{steam}(wt\%) = \frac{m_{steam}}{m_0} \cdot 100 \quad (6)$$

In order to study the effect that biomass type has on the catalysts activity and stability, the following main reactions were considered:

- Steam reforming of oxygenate compounds derived from biomass:

$$C_nH_mO_k + (n-k)H_2O \rightarrow nCO + (n+m/2-k)H_2 \quad (7)$$

- Water Gas Shift (WGS):

$$CO + H_2O \leftrightarrow CO_2 + H_2 \quad (8)$$

- Methane steam reforming:

$$CH_4 + H_2O \leftrightarrow CO + 3H_2 \quad (9)$$

- Cracking of oxygenate compounds (secondary reaction):

$$C_nH_mO_k \rightarrow \text{oxygenates} + \text{hydrocarbons} + CH_4 + CO + CO_2 \quad (10)$$

3. Results and discussion

3.1. Effect of biomass type on the distribution of pyrolysis products

3.1.1. Pyrolysis product yields

In order to evaluate the role played by biomass nature in the reforming step performance, the products obtained in the pyrolysis step were studied in detail. Biomass pyrolysis products were grouped into three different fractions: gas, liquid (bio-oil) and solid (char). Fig. 2 shows the effect that biomass type has on product distribution. The highest bio-oil yield was achieved when pine wood waste was in the feed, i.e., a bio-oil yield of 75.3 wt%. The pyrolysis of rice husk led to lower bio-oil yields (69.0 wt%) due to the higher char yield, which is directly related to the high ash (mainly silica) content of rice husk. Nevertheless, the difference is not considerable, as both biomasses are lignocellulosic. Regarding the the bio-oil yield obtained in the pyrolysis of citrus wastes (54.9 wt%), it was significantly lower than that in the pyrolysis of lignocellulosic biomasses. These differences are explained by the presence of pectin in the orange peel, whose thermal decomposition leads to high char yields (Aburto et al., 2015; Chen and Chen, 2009; Einhorn-Stoll and Kunzek, 2009; Ge et al., 2015; Sharma et al., 2001). Furthermore, the high bio-oil yields obtained in all cases are attributable to the excellent performance of the CSBR, i.e., it allows attaining short residence times of the volatiles and high heat and mass transfer rates. Consequently, devolatilization reactions are promoted and, in turn, secondary cracking reactions are minimized (Alvarez et al., 2014, 2018). The studies in the literature using other technologies under similar operating conditions report bio-oil yields in the 60–75 wt% range with pine wood wastes (Garcia-Perez et al., 2008; Oasmaa et al., 2010), in the 35–53 wt% range with citrus fruit wastes (Aguiar et al., 2008; Miranda et al., 2009) and in the 47–56 wt% range with rice husk (Guo et al., 2011; Heo et al., 2010). Concerning gas and char yields, the highest ones were obtained when citrus wastes were valorized (15.8 and 29.3 wt%, respectively). Nevertheless, the other two lignocellulosic biomasses led to similar gas and char yields: 7.3 and 17.3 wt% for pine wood and 5.8 and 25.2 wt% for rice husk, respectively. The mentioned differences in the pyrolysis product distribution have a remarkable impact on the H_2 production potential in the subsequent reforming step. Thus, the high char yields obtained in the pyrolysis of citrus wastes and rice husk hinder an efficient carbon reforming.

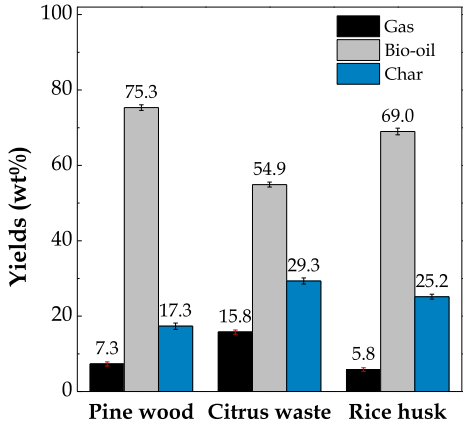

Fig. 2. Effect of biomass type on pyrolysis product distribution.

3.1.2. Pyrolysis product composition

Table 3 shows the detailed product distribution obtained in the pyrolysis of pine wood waste, citrus waste and rice husk and the main compounds of each fraction. Concerning gas composition, the gaseous fraction is mainly made up of CO and CO_2. CO_2 yield is considerably higher in the case of citrus waste compared to pine wood and rice husk. This trend is explained by the high CO_2 yield obtained in the pyrolysis of pectin (Aburto et al., 2015; Sharma et al., 2001) because pectin is basically made up of acids with carboxyl groups, which are removed by decarboxylation reactions and lead to higher amounts of CO_2 than in lignocellulosic biomasses. In the latter case, hemicellulose is the main responsible for CO_2 formation (Aburto et al., 2015; Yang et al., 2007). The yields of other compounds, such as C_1–C_4 hydrocarbons and H_2, are low in the pyrolysis of all kind of biomasses, with their overall value being below 10% the total amount of gas.

The most relevant differences are those related to bio-oil composition. The main compound of the bio-oils obtained with the feedstocks studied is water (yields between 22.4 and 25.4%), which accounts for 33.7, 40.8 and 33.4% of the total amount of the liquid in the pyrolysis of pine wood, citrus waste and rice husk, respectively. This water comes from the moisture of the biomass, as well as from the pyrolysis process by dehydration reactions (Amutio et al., 2012). Besides, higher amounts of water are produced in the pyrolysis of citrus wastes due to the water produced in the pyrolysis of the pectin contained in orange wastes

Table 3
Yields of gas, liquid and solid fractions (wt%) in the pyrolysis of different agroforestry biomass wastes.

Fraction	Compound	Pine wood	Citrus waste	Rice husk
Gas		**7.33**	**15.78**	**5.85**
	CO_2	3.27	12.31	2.55
	CO	3.38	2.72	2.95
	Others	0.68	0.75	0.35
Bio-oil		**75.33**	**54.90**	**68.99**
	Acids	2.73	3.33	7.03
	Aldehydes	1.93	–	1.98
	Alcohols	2.00	2.60	–
	Ketones	6.37	7.68	7.55
	Phenols	16.49	0.94	9.00
	Alkyl-phenols	*1.80*	*0.48*	*3.38*
	Catechols	*7.16*	*0.46*	*3.07*
	Guaiacols	*7.53*	-	*2.55*
	Ethers	–	–	2.42
	Carboxylic Anhydrides	–	–	0.91
	Furans	3.32	11.79	4.62
	Saccharides	4.46	1.58	1.10
	Nitrogenated compounds	–	0.28	1.45
	Hydrocarbons	–	0.01	–
	Others	0.06	–	–
	Unidentified	12.61	4.29	9.92
	Water	25.36	22.40	23.01
Char		**17.34**	**29.32**	**25.16**

(Aburto et al., 2015).

The bio-oil obtained in the pyrolysis of pine wood is mainly composed of phenols, which stem from the depolymerization of lignin macromolecules (Amutio et al., 2012), with their yield being of 16.49 wt %. This phenolic fraction is mainly composed of guiacols (7.53 wt%) and catechols (7.16 wt%), with a low yield of alkyl-phenols (1.80 wt%). Ketones are another relevant group in the pinewood bio-oil with a yield of 6.37 wt%, which stem from condensation reactions of the carbohydrate-derived fraction (Mohan et al., 2006) and decomposition of miscellaneous oxygenates, sugars and furans (Jacobson et al., 2013). A similar trend is observed in the pyrolysis of rice husk, given that phenols (9.00 wt%) and ketones (7.55 wt%) are also the main compounds of the bio-oil. However, the distribution of phenolic compounds obtained in the rice husk bio-oil differs from that in the pine wood one, with the yield of catechols, guaicols, and alkyl-phenols being 3.07 wt%, 2.55 wt% and 3.38 wt%, respectively. Pine wood derived bio-oil has a higher amount of saccharides, accounting for 4.46 wt% (mainly composed of levoglucosan), and a lower one of acids (2.73 wt%) compared to rice husk (1.10 and 7.03 wt% for saccharides and acids, respectively). The presence of nitrogenated compounds in the rice husk derived bio-oil is noteworthy, with their yield being 1.45 wt%. Nevertheless, the composition of the bio-oil obtained in the pyrolysis of citrus wastes is totally different. Furans are the main compounds obtained after water, with their yield being 11.79 wt% and furfural as the main compound. Ketones are the third prevailing lump with a yield of 7.68 wt % with acetone being the main compound in this group. The yield of acids (3.33 wt%) is also slightly higher than in the bio-oil from pine wood (2.73 wt%), whereas the yield of phenols is 0.94 wt%, which is extremely low compared to the bio-oil from pine wood and rice husk. Moreover, nitrogenated compounds are also evident in the bio-oil from citrus wastes, but with a lower yield compared to the one obtained from rice husk (0.28 wt% and 1.45 wt%, respectively).

The utilization of the char obtained from the pyrolysis of different agroforestry biomass wastes may improve the economic feasibility of the process (Windeatt et al., 2014). Thus, the char obtained in the pyrolysis of pine wood sawdust can be used as fuel, active carbon (after activation processes) or for soil amendment (Amutio et al., 2012), whereas the one obtained in the citrus wastes pyrolysis is more adequate to use as a fuel due to the high calorific value and low surface area (Alvarez et al., 2018). In the case of the char from rice husk, it has a high silica content, apart from the carbonaceous fraction. Therefore, it may be used for the production of either activated carbon by upgrading the carbonaceous fraction or high purity silica by controlled combustion after acid treatment (Alvarez et al., 2014).

3.2. Influence of the biomass type on the reforming step performance

3.2.1. Catalyst performance at zero time on stream

The volatiles (gas and bio-oil) obtained in the first pyrolysis step were fed in line into the second reforming step. Fig. 3 displays the initial conversion of pyrolysis volatiles and the H_2 production at zero time on stream. Although high conversions were obtained in all cases (>99.7%) and the effect of the feedstock on conversion was therefore negligible due to the relatively high space time used, the influence on H_2 production was more significant and decreased as follows: pine sawdust (11.2 wt%) > rice husk (10.0 wt%) > citrus waste (6.7 wt%). This trend is explained by the different amount of volatiles transferred into the reforming reactor. Thus, although the H_2 concentration in the gas is similar for all the feedstocks studied (around 66 vol%), the amount of gases produced changes depending on the feedstock. The reforming of the pyrolysis volatiles from pine sawdust and rice husk led to gas productions of 132.2 wt% and 119.5 wt% (based on the biomass fed into the pyrolysis process), respectively, whereas the citrus waste pyrolysis only produced 82.5 wt%. The gas produced is closely related to the amount of carbon contained in the pyrolysis volatiles, and therefore the steam reacted in the reforming process, which accounts for 49.7, 12.6 and 44.5 wt% in the reforming of pine wood, citrus waste and rice husk, respectively. Thus, the lowest gas production was obtained when citrus waste was valorized, since the carbon retained in the char is higher than in the case of the other feedstocks, and the amount of carbon to be reformed in the reforming step is therefore much lower. Likewise, Gao et al. (2018) obtained a maximum H_2 production of 10.5 wt% at 700 °C in the pyrolysis-reforming of rice husk. Moreover, papers dealing with the valorization of different agricultural biomass wastes report a H_2 production of 5.1 wt% from palm shell kernels (Akubo et al., 2019), 4.0 to 6.1 wt% from rice husk (Waheed et al., 2016), and 4.0 wt% from wood sawdust (Dong et al., 2017).

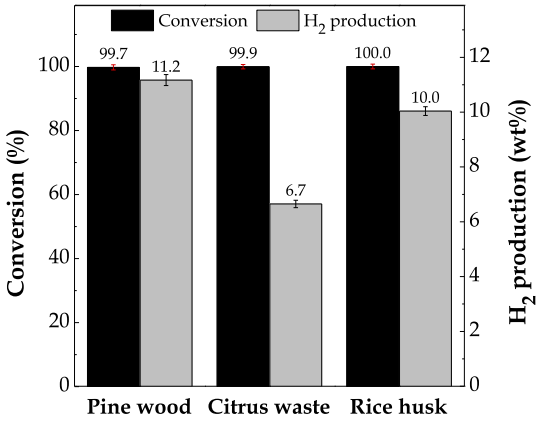

Fig. 3. Conversion and H_2 production at zero time on stream in the pyrolysis-reforming of agroforestry biomass wastes.

Fig. 4 displays the effect that feed nature has on the initial product yields. As observed, H_2, CO_2 and CO are the main compounds of the gas produced. Similar initial H_2 yields were obtained for all the biomasses studied, with their values being in the 93.5–96.4% range. Gao et al. (2018) reported H_2 yields of up to 81.1% of the stoichiometric one in the reforming of rice husk pyrolysis volatiles. Higher discrepancies are observed in the CO_2 and CO yields. The pyrolysis-reforming of citrus wastes led to the highest CO_2 yield (94.4%) and lowest CO yield (5.1%), whereas the lowest CO_2 yield (88.6%) and highest CO yield (10.6%) were attained when pine wood was valorized. As aforementioned, this trend is explained by the different nature of the feedstock, with the higher CO_2 produced in the citrus wastes being due to the pyrolysis of the pectin contained in this waste (Aburto et al., 2015; Zhou et al., 2011). Nevertheless, the reforming of rice husk pyrolysis volatiles produced CO_2 and CO yields of 92.8 and 6.8%, respectively, which are half way between those obtained for pine wood and citrus wastes. The yields of CH_4 and C_2–C_3 hydrocarbons at zero time on stream were negligible,

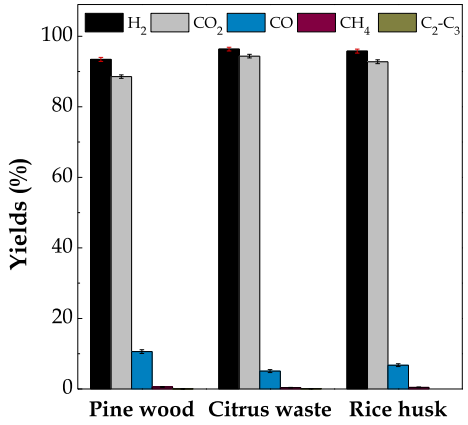

Fig. 4. Gaseous products yields at zero time on stream in the pyrolysis-reforming of agroforestry biomass wastes.

with their maximum values being of 0.56% for pine sawdust valorization and 0.09% for citrus waste valorization, respectively.

Regarding gas composition (Fig. 5), H_2 concentration in the gas was similar for all the feedstocks studied, which is around 66 vol% of the gas. Moreover, CO_2 and CO concentrations follow the same trend as CO_2 and CO yields, i.e., the highest CO_2 (32.7 vol%) and lowest CO (1.8 vol%) concentrations were obtained in the reforming of citrus waste pyrolysis volatiles, whereas the lowest CO_2 (30.2 vol%) and highest CO (3.6 vol%) concentrations corresponded to the reforming of pine sawdust pyrolysis volatiles. As aforementioned, this fact is related to the different pyrolysis volatile composition that reaches the reforming reactor; that is, the highest CO_2 yield is attained in the pyrolysis of citrus wastes (Table 3). As in the case of product yields, CH_4 and C_2–C_3 concentrations in the gas were negligible in all cases.

Similar results have also been obtained in the literature for the pyrolysis and in line reforming of rice husk, with H_2 concentrations ranging between 61.3 and 65.2 vol% (Chen et al., 2011; Pan et al., 2012; Waheed et al., 2016). A lower H_2 concentration was obtained by Al-Rahbi and Williams (2019) with waste wood pellets as feedstock, i.e., a maximum H_2 concentration of 29.7 vol%. Nevertheless, the maximum H_2 concentration obtained by Akubo et al. (2019) in the pyrolysis-reforming of sugarcane was 59.2 vol%.

3.2.2. Evolution of catalyst performance

In order to show the activity and stability of the reforming catalysts when different biomass feedstocks were treated in the pyrolysis-reforming process, the evolution of conversion and H_2 production is displayed in Fig. 6. As observed, although the initial conversion was similar for the three feedstocks studied, their evolution with time on stream was very different. The reforming of pine wood pyrolysis volatiles led to an initial conversion of 99.7% which was maintained almost steady until 60 min on stream. Afterwards, conversion decayed sharply to 57.2% when operation was conducted for 106 min on stream. In the case of citrus waste valorization, a stable conversion was observed for the first 25 min of reaction, and then decreased almost linearly with time. Finally, when rice husk was valorized, a sharp drop in volatile conversion was evident from the beginning of the reaction until 70 min on stream. For longer reaction times, conversion stabilized at around 47.5%. The differences in catalyst deactivation are related to the composition of the pyrolysis volatile stream fed into the reforming step, which heavily depends on the feedstock used. Besides, the lower bio-oil yield to be reformed when rice husks (69.0%) and, especially, citrus wastes (54.9%) were used rather than pine wood (75.3%), are evidence of the high influence of the bio-oil composition on catalyst stability (Fig. 2).

A similar trend as that of conversion was also observed for H_2 production in Fig. 6. Nevertheless, the total amount of H_2 obtained depended on the feedstock. Thus, when operation was conducted for 106 min on stream, H_2 production decreased from 11.2 to 5.7 wt%, from 6.7 to 1.3 wt% and from 10.0 to 1.1 wt% when the pyrolysis volatiles of pine wood, citrus waste and rice husk, respectively, were reformed. Furthermore, the drop in H_2 production was much more pronounced for citrus waste and rice husk than for pine wood. Thus, in the former cases, it decreased by 80.6 and 89.0%, respectively, whereas in the latter decreased by 49.1%. A similar trend for the evolution of conversion and H_2 production was also observed in the pyrolysis-reforming of pine wood sawdust on a self-prepared Ni/Al_2O_3 catalyst (Santamaria et al., 2020a). It is to note that although the reforming of pyrolysis volatile streams corresponding to different kinds of biomasses has been studied in the literature, the loss of catalyst activity has not been extensively studied under continuous operation.

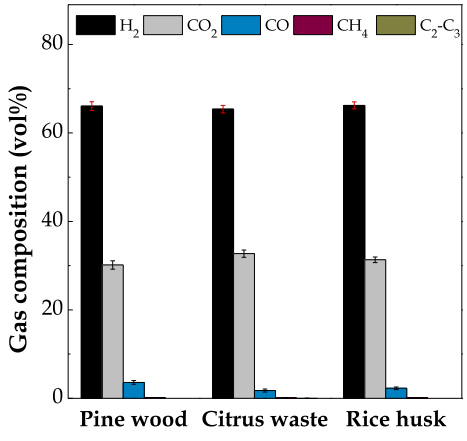

Fig. 5. Gas composition at zero time on stream in the pyrolysis-reforming of agroforestry biomass wastes.

Fig. 7 displays the evolution of product yields with time on stream for the reforming of different agroforestry wastes. H_2 yield decreased with time on stream from 93.5 to 46.4%, from 96.4 to 21.7% and from 95.8 to 11.1% for pine wood, citrus waste and rice husk, respectively, due to catalyst deactivation in the reforming and WGS reactions (Santamaria et al., 2020a). The decay of H_2 yield with time on stream followed the same trend as conversion. Regarding CO_2 yield, it decreased from 88.6 to 48.0%, from 94.4 to 41.6% and from 92.8 to 22.6% in the reforming of the volatile streams from pine wood, citrus waste and rice husk, respectively. Thus, the deactivation of the catalyst led to lower activity for the WGS reaction, which was particularly significant for citrus wastes and, especially, for rice husk. As observed in Fig. 7, the CO yield obtained when operation was conducted for 106 min on stream (the catalyst was significantly deactivated) was much higher in the reforming of the pyrolysis volatiles from rice husk (17.6%) than from pine wood (7.7%) and citrus wastes (11.3%), which is explained by the higher deactivation of the catalyst for the WGS reaction in the former case. The yields of CH_4 and C_2–C_3 hydrocarbons increased considerably with time on stream for the three feedstocks studied, which is evidence of catalyst deactivation for the reforming reaction and their production by secondary cracking reactions (Bimbela et al., 2013; Fu et al., 2014). Their values increased from 0.56 to 1.00% and from 0.04 to 0.44%, respectively, in the reforming of pine wood pyrolysis volatiles, especially in the last stages of the reaction. The increase in their yields was even more pronounced for citrus waste and rice husk, with the trends being similar for both feedstocks. The highest yields of CH_4 and C_2–C_3 hydrocarbons were obtained at the end of the run (106 min on stream) and they accounted for 3.89 and 5.03% yields for citrus waste and 3.42 and 3.68% for rice husk valorization, respectively, which are much higher than those obtained for pine wood. This is evidence that secondary cracking reactions are becoming more significant than reforming and WGS reactions when the catalyst is highly deactivated, especially for citrus waste and rice husk.

The evolution of gas composition with time on stream is shown in Fig. 8 for the reforming of different biomass pyrolysis volatiles. Although catalyst activity decreased with time on stream and the total amount of gas produced was therefore lower, the composition of the gas produced in the reforming of pine wood pyrolysis remained almost constant. This means that almost all the gases are produced by reforming, and secondary reactions, namely, cracking, decarboxylation, and decarbonilation are therefore of minor significance. Thus, H_2 and CO_2 concentrations were in the 66.1–63.5 vol% and 30.2–30.8 vol% ranges, whereas CO, CH_4 and C_2–C_3 hydrocarbon concentrations increased slightly from 3.6 to 4.9 vol%, from 0.2 to 0.6 vol% and from 0 to 0.1 vol % ranges, respectively. Fig. 8b shows the concentration of the gas obtained with time on stream in the pyrolysis-reforming of citrus waste. As observed, its trend was very different from that of pine wood. Thus, the concentration of H_2 decayed sharply from 65.4 to 38.5 vol%, and those of CO_2 and CO increased from 32.7 to 43.4 vol% and from 1.8 to 11.8 vol %, respectively, for 106 min on stream. It should be noted that high CO and CO_2 concentrations were obtained when the catalyst was

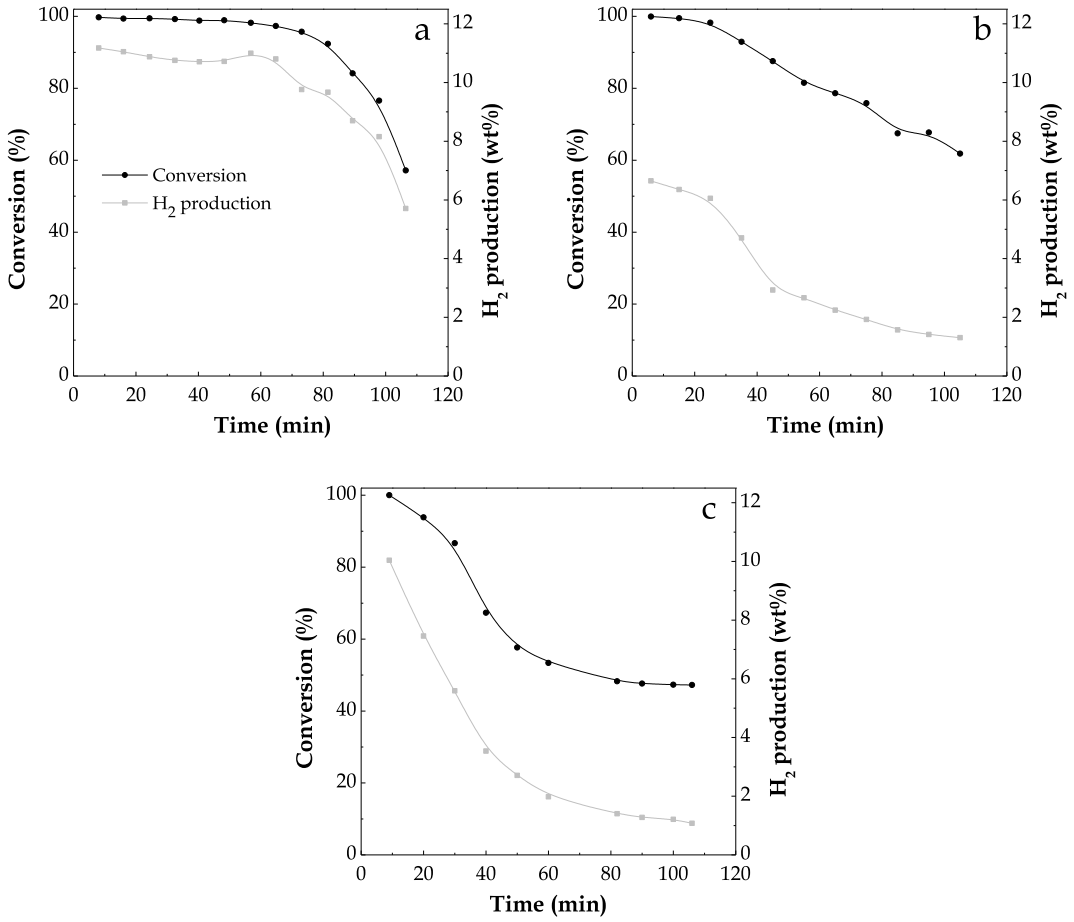

Fig. 6. Evolution of conversion and H_2 production with time on stream in the pyrolysis-reforming of pine wood (a), citrus waste (b) and rice husk (c).

deactivated, which is due to secondary cracking reactions. The evolution of the gas composition with time on stream for rice husk valorization (Fig. 8c) shows a similar trend as that obtained for citrus waste pyrolysis-reforming process. H_2 concentration decreased considerably from 66.2 to 31.7 vol%, revealing the lower extension of reforming reactions (Eq. (7)) when rice husk was used as feedstock. Furthermore, CO_2 concentration was almost constant for the whole run, in the 31.3–34.1 vol% range, whereas a sharp increase in CO concentration was observed from 2.3 to 26.6 vol%, which is evidence of catalyst deactivation for the WGS reaction. Finally, the concentrations of CH_4 and C_2–C_3 hydrocarbons increased, even though they were much lower than those of other compounds, in the 0.2–5.2 vol% and 0–2.4 vol% ranges, respectively.

As previously mentioned, the composition of the pyrolysis volatile stream changes depending on the feedstock, which greatly influences catalyst stability in the reforming step. In this regard, the bio-oil derived from pine wood had a higher content of phenols (especially guaicols and catechols) and saccharides than that from citrus waste and rice husk. These compounds are well known for being the main coke precursors in the steam reforming of biomass derived compounds (Fernandez et al., 2022b; Ochoa et al., 2017; Remón et al., 2015). However, despite the bio-oils derived from citrus waste and rice husk had much lower concentrations of these compounds, the deactivation rate of the catalysts involved was significantly higher than in the reforming of pine wood pyrolysis volatiles. In the case of citrus waste, furans (mainly furfural) were the main compounds in the bio-oil. In this regard, furfural has been reported to cause severe catalyst deactivation in steam reforming reactions (Remón et al., 2015; Trane-Restrup and Jensen, 2015). Concerning the rice husk derived bio-oil, the high yield of carboxylic acids (7.03 wt%) greatly influences the stability of the catalysts due to their low reactivity in reforming reactions (Li et al., 2018; Remón et al., 2015). Furthermore, the presence of N-containing species in the bio-oils from both citrus waste and rice husk (0.28 and 1.45 wt%, respectively), may involve a high catalyst deactivation rate (Ren et al., 2021). Thus, the N contained in the biomass feedstock was converted during the pyrolysis process in N-containing compounds, namely, pyrrole-N, pyridine-N and nitrile-N, which can be further decomposed into NO_x precursors (mainly NH_3, HCN and HNCO) (Cao et al., 2014; Chen et al., 2023; Leppälahti, 1995). The distribution of these products depends on the chemical composition of the feedstock and reaction temperature (Binte Mohamed et al., 2022; Torres et al., 2007), with NH_3 formation being favored at low temperatures (Binte Mohamed et al., 2022; Chen et al., 2023). Moreover, it is well-established that Ni based catalysts are effective to convert HCN into NH_3 by hydrogenation (Eq. (11)) and subsequent decomposition of NH_3 into N_2 and H_2 (Eq. (12)) (Kumagai et al., 2017, 2020).

$$HCN + 3H_2 \rightarrow NH_3 + CH_4 \quad (11)$$

$$2NH_3 \rightarrow N_2 + 3H_2 \quad (12)$$

The reforming activity of Ni catalysts is compromised by this latter reaction due to the adsorption of NH_3 on the Ni active sites (Binte Mohamed et al., 2022; Yin et al., 2020), which means that both NH_3 decomposition and reforming are competing reactions. This fact explains the fast catalyst deactivation and the evolution of the yields and compositions of the products when citrus waste and, especially rice husk, were valorized.

3.2.3. *Discussion on the origin of catalyst deactivation*

Several research studies dealing with the pyrolysis and in line reforming of biomass (Nahil et al., 2013; Santamaria et al., 2019),

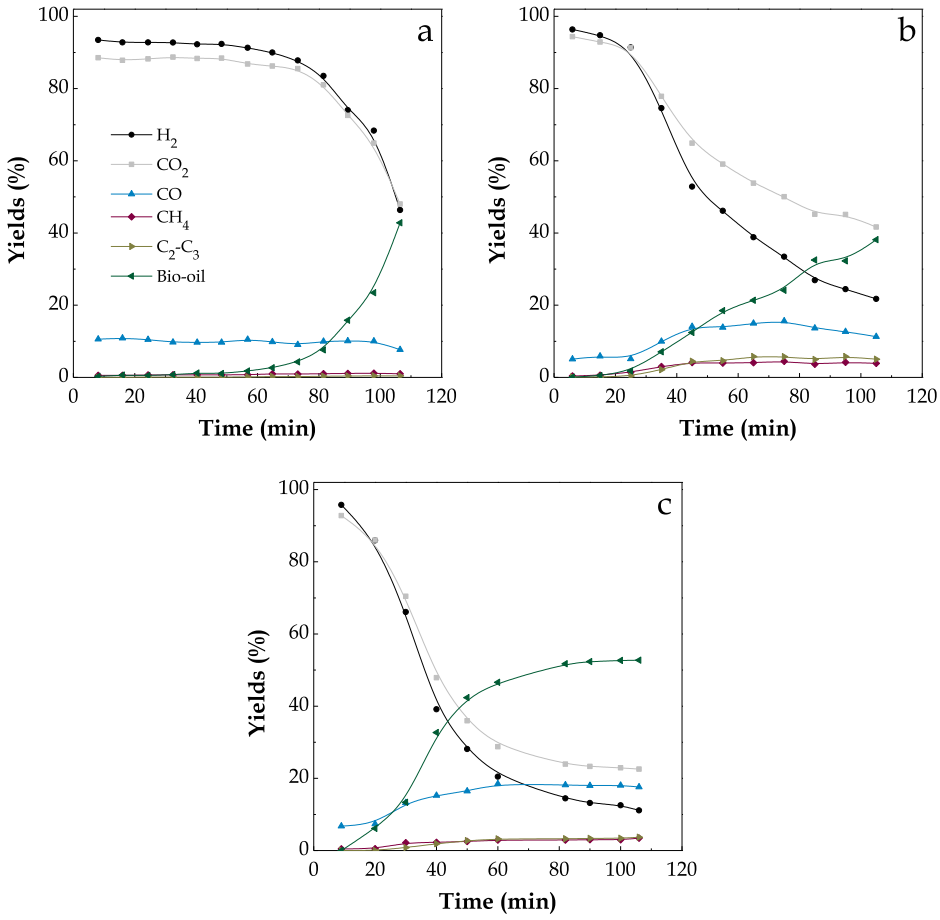

Fig. 7. Evolution of product yields with time on stream in the pyrolysis-reforming of pine wood (a), citrus waste (b) and rice husk (c).

reforming of oxygenated compounds (Vicente et al., 2014) and bio-oil reforming processes (Remiro et al., 2013) have reported metal sintering and, especially, coke deposition, as the main cause of catalyst deactivation. Moreover, reforming catalysts may also be deactivated by oxidation of the metal active phase or by poisoning due to the presence of inorganic impurities in the biomass, such as sulfur, organic nitrogen compounds, phosphates or chloride species (Ashok et al., 2019). It should be noted that, frequently, the combination of more than one of the above mechanisms is responsible for the catalyst deactivation.

In order to identify the main causes of catalyst deactivation, the spent catalyst samples were characterized by N_2 adsorption–desorption, XRD, ultimate analysis, TPO, and TEM images. Table 4 shows the textural properties of the fresh reduced and deactivated catalysts. As observed, there was a decrease in the specific surface area and pore volume in all the samples due to the blockage of the catalyst pores by coke deposition, whereas the mean diameter of the catalyst pores increased by the blockage of the smaller pores. In the case of pine wood, this blockage was less pronounced (BET surface area slightly decreases from 19.0 $m^2\ g^{-1}$ to 17.1 $m^2\ g^{-1}$) and did not lead to a complete clogging of the catalyst surface. However, when citrus waste and rice husk were valorized, a more severe blockage was observed in both deactivated samples, leading to a considerable reduction in S_{BET} and pore volume (S_{BET} decreased from 19.0 to 6.4 and 6.0 $m^2\ g^{-1}$ and pore volume from 0.111 to 0.028 and 0.026 $cm^3\ g^{-1}$ for citrus waste and rice husk, respectively). These results suggest that a different type of coke was deposited on the catalysts when pine wood or citrus waste and rice husk are used as feedstock. Moreover, the full blockage of the catalyst pores observed in the citrus waste and rice husk valorization may be related to the rapid loss of catalyst activity (Fig. 6). Thus, this drastic blockage of the support pores hinders the access of the reactants to the active sites, involving the fast deactivation of the reforming catalyst.

Fig. 9 shows the XRD profiles of both fresh reduced and deactivated catalysts when different biomasses were valorized by the pyrolysis-reforming process. This analysis was conducted in order to ascertain, on the one hand, any possible change in the metallic structure of the samples and, on the other hand, whether metal sintering occurred leading to catalyst deactivation. As observed, there are no significant differences in the profiles, with all showing typical diffraction peaks corresponding to Ni^0, $CaAl_2O_4$, Al_2O_3, $CaO(Al_2O_3)_2$ and $CaAl_{12}O_{19}$. It is to note that NiO crystalline phase was not detected in any of the XRD patterns, which discards oxidation of Ni^0 sites as the main cause of catalyst decay in all the runs. Moreover, the Ni^0 crystallite size in all samples was determined by Debye-Scherrer equation at $2\theta = 52°$. The fresh catalyst showed a Ni^0 crystallite size of 25 nm, whereas a similar slight increase was observed in all the catalysts deactivated for 106 min on stream. Thus, it may be concluded that catalyst decay is not due to Ni sintering.

Ultimate analysis of the deactivated samples was conducted in order to determine the possible amount of sulfur in the catalyst. As previously mentioned, the impurities in each type of biomass may lead to a fast catalyst deactivation. It is to note that most of these compounds remained in the char produced in the first pyrolysis step, which, as stated before, was continuously removed by a lateral outlet (Fig. 1). The results show that the amount of sulfur in the catalysts decreases as follows: Citrus waste (0.32 wt%) > Rice husk (0.25 wt%) > Pine wood (0.21 wt%.). This means that the concentration of sulfur compounds in the volatile stream accounts for 2.69 ppmv for the pine wood, 3.60 ppmv for the rice husk and 6.74 ppmv for the citrus wastes. Furthermore, it has been reported that small concentrations of sulfur compounds may significantly affect the catalyst performance during steam reforming

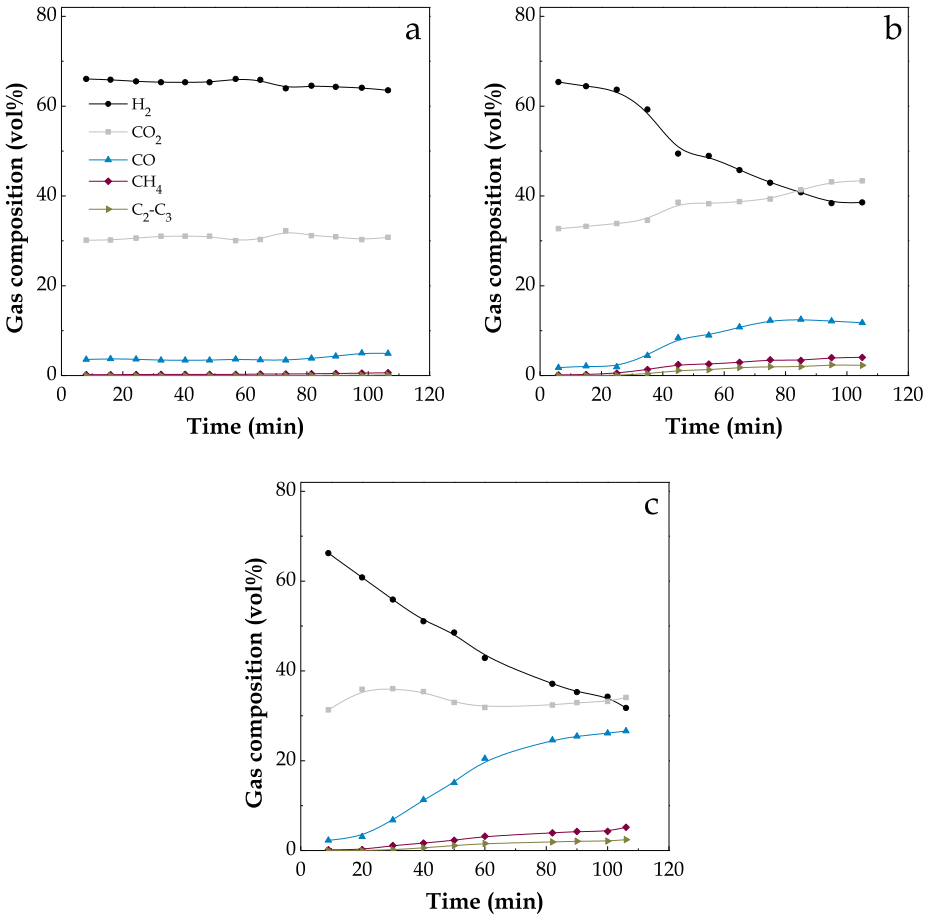

Fig. 8. Evolution of gas composition with time on stream in the pyrolysis-reforming of pine wood (a), citrus waste (b) and rice husk (c).

Table 4
Properties of the fresh and deactivated catalysts in the pyrolysis-reforming of agroforestry biomass wastes.

Feedstock	S_{BET} [a] ($m^2\ g^{-1}$)	V_{pore} [b] ($cm^3\ g^{-1}$)	d_{pore} [b] (Å)
Fresh catalyst	19.0	0.111	122
Pine wood	17.1	0.101	243
Citrus waste	6.4	0.028	208
Rice husk	6.0	0.026	251

[a] S_{BET}: Specific surface area determined by Brunauer–Emmett–Teller (BET) method.
[b] V_{pore} and d_{pore}: pore volume and pore diameter distribution determined by Barret–Joyner–Halenda (BJH) method.

reactions (Koningen and Sjöström, 1998), especially when citrus wastes are valorized. However, given the low concentration of sulfur compounds in the volatile stream, poisoning of the metal active sites has not been considered as the main cause of catalyst decay.

In order to analyze the coke deposited on the deactivated catalysts, temperature programmed oxidation (TPO) was conducted. This technique allows determining both the amount of coke and its nature/location on the catalyst surface. Thus, Fig. 10 shows the TPO profiles and Table 5 the coke content and average coke deposition rate obtained for the three feedstocks studied. As observed in Fig. 10, there are two clear peaks at 425 and 563 °C in the catalyst used for pine wood valorization, which correspond to two types of cokes differing in their structure and/or location. The first peak corresponds to either an amorphous coke or one that is located on the Ni particles, whose combustion is promoted by Ni catalytic effect. The second peak is a structured coke and/or

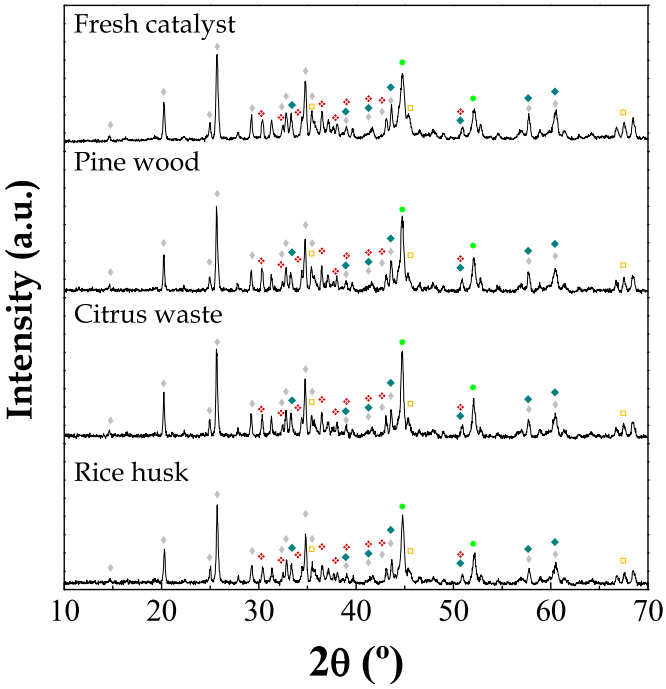

Fig. 9. XRD patterns of the fresh reduced catalyst and those deactivated in the steam reforming of pyrolysis volatiles from agroforestry biomass wastes. Crystalline phases: (◖) $CaO(Al_2O_3)_2$, (●) Ni^0, (❖) $CaAl_2O_4$, (◆) $CaAl_{12}O_{19}$, and (□) Al_2O_3.

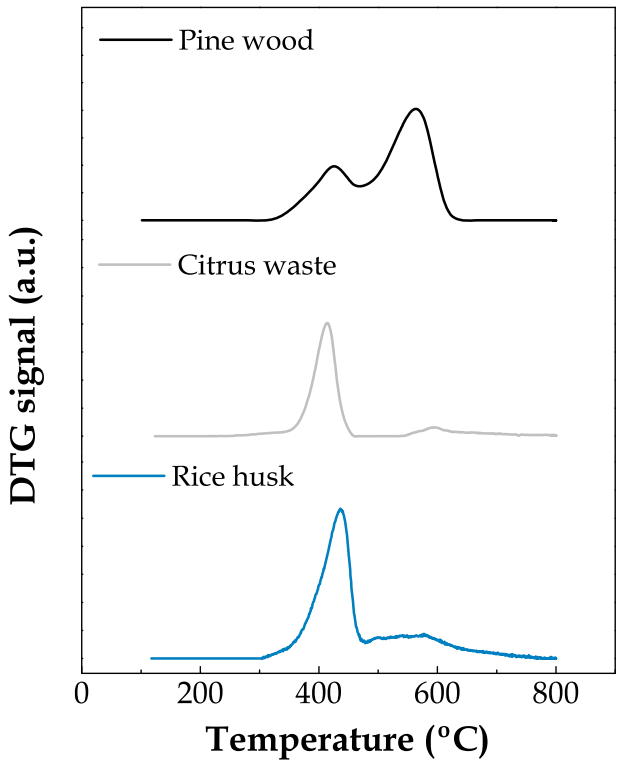

Fig. 10. Temperature programmed oxidation (TPO) profiles of the catalysts deactivated in the pyrolysis-reforming of different agroforestry biomass wastes.

Table 5
Coke content (C_C) and average coke deposition rate (r_C) in the catalyst used in the pyrolysis-reforming of agroforestry biomass wastes.

Feedstock	Coke deposition	
	C_C (wt%)	r_C ($mg_{coke}\ g_{cat}^{-1}\ g_{biomass}^{-1}$)
Pine wood	4.65	0.59
Citrus waste	2.91	0.37
Rice husk	3.37	0.42

deposited far from the Ni particles. Nevertheless, the TPO profiles obtained for citrus wastes and rice husk are different, since only one main peak is observed at low temperature and corresponds to amorphous coke. This type of coke has been reported as the main cause of catalyst deactivation, since it encapsulates Ni particles, hindering the access of reactants to the active sites (Landa et al., 2022; Santamaria et al., 2020b). In the case of citrus waste valorization, the combustion of the amorphous coke occurs mainly at around 414 °C, even though a small peak appears at around 584 °C. This second peak is very low compared to the first peak, which is evidence of the different performance of the catalyst in the reforming process. A similar profile was obtained in the catalyst deactivated in the reforming of rice husk pyrolysis volatiles, with the main peak being at around 430 °C, which corresponds to the coke deposited on Ni metallic sites, and a small one at higher temperature. These results are consistent with the ones obtained in the N_2 adsorption-desorption technique, wherein a more severe blockage of the catalyst pores was observed in the catalysts used in the citrus waste and rice husk pyrolysis-reforming runs.

Regarding the amount of coke and average deposition rate on the catalysts (Table 5), it is noteworthy that despite the lower deactivation rate observed in the pine wood run (Figs. 6 and 7), the highest amount of coke was deposited on this catalyst (4.65 wt% for pine wood vs. 2.91 wt % and 3.37 wt% for citrus waste and rice husk, respectively). These results are evidence of the higher influence of coke nature and location than its content on catalyst deactivation. Thus, although the same catalyst and operating conditions were used for the pyrolysis-reforming process with the three feedstocks, the composition of the pyrolysis volatile stream greatly influenced the type of coke deposited on the catalysts. Thus, a fast deactivation was observed when citrus waste and rice husk were valorized.

In order to analyze the morphology of the coke deposited on the deactivated catalysts, transmission electron microscopy (TEM) was performed and the images are displayed in Fig. 11. The dark areas are ascribed to Ni particles and the grey shapes to the support.

As observed, no specific morphology of the coke is evidenced in any catalyst, i.e., it corresponds to an amorphous coke. Therefore, the presence of filamentous coke was not observed, which is consistent with previous results in which biomass pyrolysis and in line steam reforming were analyzed (Arregi et al., 2018b; Santamaria et al., 2019). It is to note that the coke deposited on the catalysts used in the citrus waste and rice husk valorization (blurred spots) is clearly located on the Ni crystallite sites, thereby hindering the access of reactants to the active sites. These images are consistent with the results obtained by the N_2 adsorption-desorption technique (severe blockage of the catalyst pores in the catalysts used with citrus waste and rice husk) and by TPO (a single peak burning at low temperature ascribed to encapsulating coke). These results are evidence that, although the cokes in all the catalysts are of amorphous nature, their condensation degree and location, and therefore the blockage of Ni sites, is influenced by the composition of the volatile stream to be reformed.

Accordingly, the main cause of catalyst decay in the pine wood valorization is coke deposition, with phenolic compounds, especially guiacols and catechols, being the main coke precursors. In the citrus waste and rice husk pyrolysis-reforming, catalyst deactivation may not be a consequence of a single mechanism, but the combination of multiple factors. Accordingly, the composition of the volatiles derived from citrus waste and rice husk pyrolysis, with a high concentration of furans in the former case and N-containing compounds in both cases, may be responsible for the fast catalyst decay. On the one hand, these compounds lead to the formation of encapsulating coke, which severely blocks the catalyst pores, hindering the access of reactants to Ni sites. On the other hand, as mentioned above, the presence of N-containing impurities in these bio-oils (0.28 and 1.45 wt% in citrus waste and rice husk, respectively) may involve the formation of NOx precursors, whose decomposition competes with the reforming reaction due to the adsorption of NH_3 on Ni active sites, thereby leading to a fast catalyst deactivation.

4. Conclusions

The pyrolysis and in line steam reforming conducted in a conical spouted bed-fluidized bed configuration has proven to be a suitable and flexible strategy for the production of H_2 from different agroforestry residues.

The diverse composition of the pyrolysis volatiles, depending on the feedstock, involves significant differences in both the initial reaction indices and the catalyst stability throughout the reaction. Thus, although initial conversions were higher than 99% for the three biomasses studied, the initial H_2 production decreased as follows: Pine wood (11.2 wt%) > rice husk (10.0 wt%) > citrus waste (6.7 wt%). Moreover, the differences observed regarding catalyst deactivation are evidence of the high influence of bio-oil composition on catalyst stability. Pine wood processing leads to full conversion for 60 min on stream followed by a sharp decrease. However, the valorization of citrus waste involves a severe deactivation subsequent to 25 min on stream, with this fact being even more pronounced when rice husk was valorized (volatile conversion sharply decreases from the beginning of the reaction).

The assessment of the main deactivation causes allows excluding metal sintering or Ni active site oxidation as responsible of catalyst decay. Although sulfur poisoning may affect the catalyst performance, it

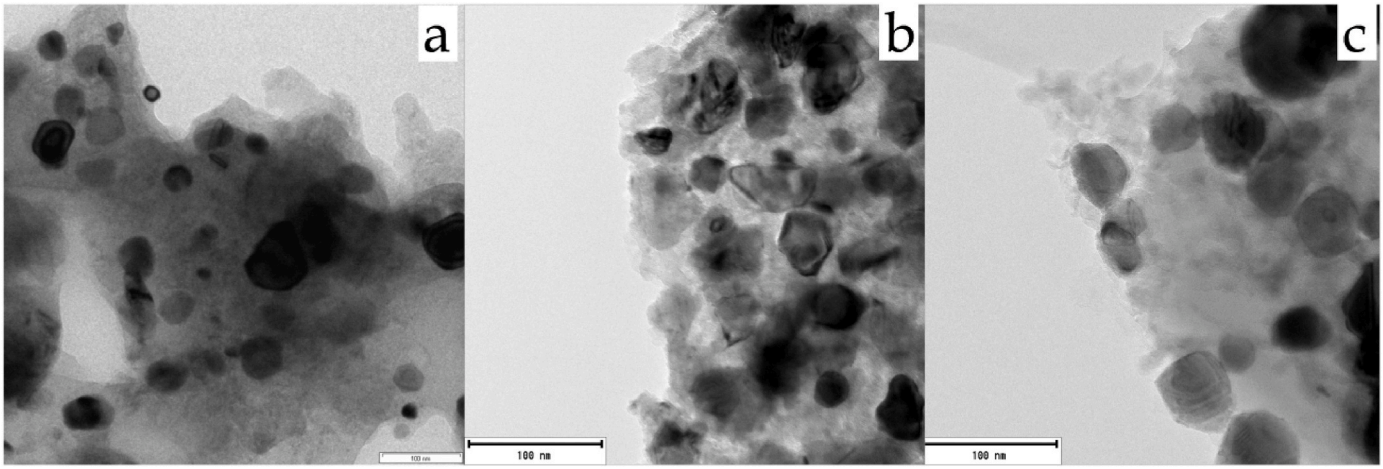

Fig. 11. Transmission electron microscopy (TEM) images of the catalysts deactivated in the reforming of pyrolysis volatiles from pine wood (a), citrus waste (b) and rice husk (c).

was also discarded due to the low concentration of sulfur compounds in the volatile stream.

In all pyrolysis-reforming runs, coke deposition greatly affected the catalyst performance during the reaction. Furthermore, differences in the nature and location of the coke, due to differences in the pyrolysis volatile composition, had an influence on the reforming catalyst stability. Thus, phenolic compounds, particularly guaiacols and catechols, are the main coke precursors in the pine wood valorization. However, the higher concentration of furans in the citrus waste bio-oil and N-containing compounds in the bio-oils from both citrus waste and rice husk, involve the formation of an encapsulating coke, which severely clogs the catalyst pores, and therefore leads to more severe deactivation than that deposited on the catalyst used in the pine wood pyrolysis-reforming. Although all the cokes deposited on the deactivated catalysts have an amorphous nature, coke nature and location rather than its content play a key role in catalyst deactivation. Moreover, the formation of NOx precursors from N-containing compounds in these pyrolysis volatiles competes with the reforming reaction by the adsorption of NH_3 on Ni active sites, thereby leading to fast catalyst deactivation.

The results of this study involve a step further on the knowledge of the role played by bio-oil composition in the deactivation of the reforming catalysts and allow the proposal of future strategies for enhancing catalyst stability in the reforming stage.

Credit author statement

Aitor Arregi[a]: Investigation, Writing – original draft, Visualization, Writing – review and editing, **Laura Santamaria[a]** Validation, Writing – original draft, Visualization, Writing – review and editing; **Gartzen Lopez[a,b]:** Conceptualization, Validation, Writing – review and editing, Visualization, Supervision, Project administration; **Martin Olazar[a]:** Writing – review and editing, Visualization, Supervision, Project administration, Funding acquisition; **Javier Bilbao[a]:** Writing – review and editing, Visualization, Supervision, Project administration, Funding acquisition; **Maite Artetxe[a]:** Conceptualization, Writing – review and editing, Visualization, Supervision, Project administration, Funding acquisition; **Maider Amutio[a]:** Conceptualization, Writing – review and editing, Visualization, Supervision, Project administration, Funding acquisition.

Declaration of competing interest

The authors declare that they have no known competing financial interests or personal relationships that could have appeared to influence the work reported in this paper.

Data availability

Data will be made available on request.

Acknowledgments

This work was carried out with the financial support of the grants PID2022-140704OB-I00 and PID2022-139454OB-I00 funded by MCIU/AEI/10.13039/501100011033 and “ERDF, a way of making Europe”, the grants TED 2021-132056B–I00 and PLEC 2021-008062 funded by MCIN/AEI/10.13039/501100011033 and “European Union NextGenerationEU/PRTR”, and the grants IT1645-22 and KK-2023/00060 funded by the Basque Government. Moreover, this project has received funding from the European Union’s Horizon 2020 research and innovation programme under the Marie Sklodowska-Curie grant agreement No. 823745.

Appendix A. Supplementary data

Supplementary data to this article can be found online at https://doi.org/10.1016/j.jenvman.2023.119071.

References

Aburto, J., Moran, M., Galano, A., Torres-García, E., 2015. Non-isothermal pyrolysis of pectin: a thermochemical and kinetic approach. J. Anal. Appl. Pyrolysis 112, 94–104. https://doi.org/10.1016/j.jaap.2015.02.012.

Aguiar, L., Márquez-Montesinos, F., Gonzalo, A., Sánchez, J.L., Arauzo, J., 2008. Influence of temperature and particle size on the fixed bed pyrolysis of orange peel residues. J. Anal. Appl. Pyrolysis 83, 124–130. https://doi.org/10.1016/j.jaap.2008.06.009.

Akubo, K., Nahil, M.A., Williams, P.T., 2019. Pyrolysis-catalytic steam reforming of agricultural biomass wastes and biomass components for production of hydrogen/syngas. J. Energy Inst. 92, 1987–1996. https://doi.org/10.1016/j.joei.2018.10.013.

Al-Rahbi, A.S., Williams, P.T., 2019. Waste ashes as catalysts for the pyrolysis–catalytic steam reforming of biomass for hydrogen-rich gas production. J. Mater. Cycles Waste Manag. 21, 1224–1231. https://doi.org/10.1007/s10163-019-00876-8.

Alvarez, J., Lopez, G., Amutio, M., Bilbao, J., Olazar, M., 2014. Bio-oil production from rice husk fast pyrolysis in a conical spouted bed reactor. Fuel 128, 162–169. https://doi.org/10.1016/j.fuel.2014.02.074.

Alvarez, J., Hooshdaran, B., Cortazar, M., Amutio, M., Lopez, G., Freire, F.B., Haghshenasfard, M., Hosseini, S.H., Olazar, M., 2018. Valorization of citrus wastes by fast pyrolysis in a conical spouted bed reactor. Fuel 224, 111–120. https://doi.org/10.1016/j.fuel.2018.03.028.

Amutio, M., Lopez, G., Artetxe, M., Elordi, G., Olazar, M., Bilbao, J., 2012. Influence of temperature on biomass pyrolysis in a conical spouted bed reactor. Resour. Conserv. Recycl. 59, 23–31. https://doi.org/10.1016/j.resconrec.2011.04.002.

Arregi, A., Amutio, M., Lopez, G., Artetxe, M., Alvarez, J., Bilbao, J., Olazar, M., 2017. Hydrogen-rich gas production by continuous pyrolysis and in-line catalytic reforming of pine wood waste and HDPE mixtures. Energy Convers. Manag. 136, 192–201. https://doi.org/10.1016/j.enconman.2017.01.008.

Arregi, A., Amutio, M., Lopez, G., Bilbao, J., Olazar, M., 2018a. Evaluation of thermochemical routes for hydrogen production from biomass: a review. Energy Convers. Manag. 165, 696–719. https://doi.org/10.1016/j.enconman.2018.03.089.

Arregi, A., Lopez, G., Amutio, M., Artetxe, M., Barbarias, I., Bilbao, J., Olazar, M., 2018b. Role of operating conditions in the catalyst deactivation in the in-line steam reforming of volatiles from biomass fast pyrolysis. Fuel 216, 233–244. https://doi.org/10.1016/j.fuel.2017.12.002.

Arregi, A., Lopez, G., Amutio, M., Barbarias, I., Bilbao, J., Olazar, M., 2016. Hydrogen production from biomass by continuous fast pyrolysis and in-line steam reforming. RSC Adv. 6, 25975–25985. https://doi.org/10.1039/c6ra01657j.

Arregi, A., Lopez, G., Amutio, M., Barbarias, I., Santamaria, L., Bilbao, J., Olazar, M., 2018c. Kinetic study of the catalytic reforming of biomass pyrolysis volatiles over a commercial Ni/Al_2O_3 catalyst. Int. J. Hydrogen Energy 43, 12023–12033. https://doi.org/10.1016/j.ijhydene.2018.05.032.

Arregi, A., Lopez, G., Amutio, M., Barbarias, I., Santamaria, L., Bilbao, J., Olazar, M., 2018d. Regenerability of a Ni catalyst in the catalytic steam reforming of biomass pyrolysis volatiles. J. Ind. Eng. Chem. 68, 69–78. https://doi.org/10.1016/j.jiec.2018.07.030.

Ashok, J., Das, S., Dewangan, N., Kawi, S., 2019. H_2S and NO_x tolerance capability of CeO_2 doped $La_{1-x}Ce_xCo_{0.5}Ti_{0.5}O_{3-\delta}$ perovskites for steam reforming of biomass tar model reaction. Energy Convers. Manag. X 1, 100003. https://doi.org/10.1016/j.ecmx.2019.100003.

Barbarias, I., Artetxe, M., Lopez, G., Arregi, A., Bilbao, J., Olazar, M., 2018. Influence of the conditions for reforming HDPE pyrolysis volatiles on the catalyst deactivation by coke. Fuel Process. Technol. 171, 100–109. https://doi.org/10.1016/j.fuproc.2017.11.003.

Barbarias, I., Lopez, G., Artetxe, M., Arregi, A., Santamaria, L., Bilbao, J., Olazar, M., 2016. Pyrolysis and in-line catalytic steam reforming of polystyrene through a two-step reaction system. J. Anal. Appl. Pyrolysis 122, 502–510. https://doi.org/10.1016/j.jaap.2016.10.006.

Bimbela, F., Oliva, M., Ruiz, J., García, L., Arauzo, J., 2013. Hydrogen production via catalytic steam reforming of the aqueous fraction of bio-oil using nickel-based coprecipitated catalysts. Int. J. Hydrogen Energy 38, 14476–14487. https://doi.org/10.1016/j.ijhydene.2013.09.038.

Binte Mohamed, D.K., Veksha, A., Ha, Q.L.M., Chan, W.P., Lim, T., Lisak, G., 2022. Advanced Ni tar reforming catalysts resistant to syngas impurities: current knowledge, research gaps and future prospects. Fuel 318, 123602. https://doi.org/10.1016/j.fuel.2022.123602.

Bushra, B., Remya, N., 2020. Biochar from pyrolysis of rice husk biomass—characteristics, modification and environmental application. Biomass Convers. Biorefin. https://doi.org/10.1007/s13399-020-01092-3. Article (in press).

Cai, W., Kang, N., Jang, M.K., Sun, C., Liu, R., Luo, Z., 2019. Long term storage stability of bio-oil from rice husk fast pyrolysis. Energy 186, 115882. https://doi.org/10.1016/j.energy.2019.115882.

Caldeira, C., Vlysidis, A., Fiore, G., De Laurentiis, V., Vignali, G., Sala, S., 2020. Sustainability of food waste biorefinery: a review on valorisation pathways, techno-economic constraints, and environmental assessment. Bioresour. Technol. 312, 123575 https://doi.org/10.1016/j.biortech.2020.123575.

Cao, J.P., Liu, T.L., Ren, J., Zhao, X.Y., Wu, Y., Wang, J.X., Ren, X.Y., Wei, X.Y., 2017. Preparation and characterization of nickel loaded on resin char as tar reforming catalyst for biomass gasification. J. Anal. Appl. Pyrolysis 127, 82–90. https://doi.org/10.1016/j.jaap.2017.08.020.

Cao, J.P., Shi, P., Zhao, X.Y., Wei, X.Y., Takarada, T., 2014. Catalytic reforming of volatiles and nitrogen compounds from sewage sludge pyrolysis to clean hydrogen and synthetic gas over a nickel catalyst. Fuel Process. Technol. 123, 34–40. https://doi.org/10.1016/j.fuproc.2014.01.042.

Chang, S.H., 2020. Rice husk and its pretreatments for bio-oil production via fast pyrolysis: a review. Bioenergy Res 13, 23–42. https://doi.org/10.1007/s12155-019-10059-w.

Chen, B., Chen, Z., 2009. Sorption of naphthalene and 1-naphthol by biochars of orange peels with different pyrolytic temperatures. Chemosphere 76, 127–133. https://doi.org/10.1016/j.chemosphere.2009.02.004.

Chen, H., Shan, R., Zhao, F., Gu, J., Zhang, Y., Yuan, H., Chen, Y., 2023. A review on the NOx precursors release during biomass pyrolysis. Chem. Eng. J. 451, 138979 https://doi.org/10.1016/j.cej.2022.138979.

Chen, T., Wu, C., Liu, R., 2011. Steam reforming of bio-oil from rice husks fast pyrolysis for hydrogen production. Bioresour. Technol. 102, 9236–9240. https://doi.org/10.1016/j.biortech.2011.07.033.

Cormos, C., 2023. Green hydrogen production from decarbonized biomass gasification: an integrated techno-economic and environmental analysis. Energy 270, 126926. https://doi.org/10.1016/j.energy.2023.126926.

Cristóbal, J., Caldeira, C., Corrado, S., Sala, S., 2018. Techno-economic and profitability analysis of food waste biorefineries at European level. Bioresour. Technol. 259, 244–252. https://doi.org/10.1016/j.biortech.2018.03.016.

De Laurentiis, V., Corrado, S., Sala, S., 2018. Quantifying household waste of fresh fruit and vegetables in the EU. Waste Manage. (Tucson, Ariz.) 77, 238–251. https://doi.org/10.1016/j.wasman.2018.04.001.

Dong, L., Wu, C., Ling, H., Shi, J., Williams, P.T., Huang, J., 2017. Promoting hydrogen production and minimizing catalyst deactivation from the pyrolysis-catalytic steam reforming of biomass on nanosized NiZnAlOx catalysts. Fuel 188, 610–620. https://doi.org/10.1016/j.fuel.2016.10.072.

Einhorn-Stoll, U., Kunzek, H., 2009. The influence of the storage conditions heat and humidity on conformation, state transitions and degradation behaviour of dried pectins. Food Hydrocolloids 23, 856–866. https://doi.org/10.1016/j.foodhyd.2008.05.001.

Fernandez, E., Amutio, M., Artetxe, M., Arregi, A., Santamaria, L., Lopez, G., Bilbao, J., Olazar, M., 2021. Assessment of product yields and catalyst deactivation in fixed and fluidized bed reactors in the steam reforming of biomass pyrolysis volatiles. Process Saf. Environ. Protect. 145, 52–62. https://doi.org/10.1016/j.psep.2020.07.039.

Fernandez, E., Cortazar, M., Santamaria, L., Artetxe, M., Amutio, M., Lopez, G., Bilbao, J., Olazar, M., 2022a. Tuning pyrolysis temperature to improve the in-line steam reforming catalyst activity and stability. Process Saf. Environ. Protect. 166, 440–450. https://doi.org/10.1016/j.psep.2022.08.039.

Fernandez, E., Santamaria, L., Artetxe, M., Amutio, M., Arregi, A., Lopez, G., Bilbao, J., Olazar, M., 2022b. Conditioning the volatile stream from biomass fast pyrolysis for the attenuation of steam reforming catalyst deactivation. Fuel 312, 122910. https://doi.org/10.1016/j.fuel.2021.122910.

Freitas, L.C., Barbosa, J.R., da Costa, A.L.C., Bezerra, F.W.F., Pinto, R.H.H., Carvalho Junior, R.N.d., 2021. From waste to sustainable industry: how can agro-industrial wastes help in the development of new products? Resour. Conserv. Recycl. 169, 105466 https://doi.org/10.1016/j.resconrec.2021.105466.

Fu, P., Yi, W., Li, Z., Bai, X., Zhang, A., Li, Y., Li, Z., 2014. Investigation on hydrogen production by catalytic steam reforming of maize stalk fast pyrolysis bio-oil. Int. J. Hydrogen Energy 39, 13962–13971. https://doi.org/10.1016/j.ijhydene.2014.06.165.

Galvagno, A., Prestipino, M., Maisano, S., Urbani, F., Chiodo, V., 2019. Integration into a citrus juice factory of air-steam gasification and CHP system: energy sustainability assessment. Energy Convers. Manag. 193, 74–85. https://doi.org/10.1016/j.enconman.2019.04.067.

Gao, N., Quan, C., Ma, Z., Wu, C., 2018. Thermal characteristics of biomass pyrolysis oil and potential hydrogen production by catalytic steam reforming. Energy Fuels 32, 5234–5243. https://doi.org/10.1021/acs.energyfuels.8b00365.

Garcia-Perez, M., Wang, X.S., Shen, J., Rhodes, M.J., Tian, F., Lee, W.-., Wu, H., Li, C.-., 2008. Fast pyrolysis of oil mallee woody biomass: effect of temperature on the yield and quality of pyrolysis products. Ind. Eng. Chem. Res. 47, 1846–1854. https://doi.org/10.1021/ie071497p.

Ge, S., Xu, Y., Tian, Z., She, S., Huang, L., Zhang, Z., Hu, Y., Weng, J., Cao, M., Sheng, L., 2015. Pyrolysis study of pectin by tunable synchrotron vacuum ultraviolet photoionization mass spectrometry. J. Therm. Anal. Calorim. 120, 1399–1405. https://doi.org/10.1007/s10973-015-4440-4.

Guo, X., Wang, S., Wang, Q., Guo, Z., Luo, Z., 2011. Properties of bio-oil from fast pyrolysis of rice husk. Chin. J. Chem. Eng. 19, 116–121. https://doi.org/10.1016/S1004-9541(09)60186-5.

Heo, H.S., Park, H.J., Dong, J., Park, S.H., Kim, S., Suh, D.J., Suh, Y., Kim, S., Park, Y., 2010. Fast pyrolysis of rice husk under different reaction conditions. J. Ind. Eng. Chem. 16, 27–31. https://doi.org/10.1016/j.jiec.2010.01.026.

Jacobson, K., Maheria, K.C., Kumar Dalai, A., 2013. Bio-oil valorization: a review. Energy Fuels 23, 91–106. https://doi.org/10.1016/j.rser.2013.02.036.

Jeong, D., Park, H., Jang, B., Ju, Y., Shin, M.H., Oh, E.J., Lee, E.J., Kim, S.R., 2021. Recent advances in the biological valorization of citrus peel waste into fuels and chemicals. Bioresour. Technol. 323, 124603 https://doi.org/10.1016/j.biortech.2020.124603.

Khademi, M.H., Lotfi-Varnoosfaderani, M., 2021. Sustainable ammonia production from steam reforming of biomass-derived glycerol in a heat-integrated intensified process: modeling and feasibility study. J. Clean. Prod. 324, 129241 https://doi.org/10.1016/j.jclepro.2021.129241.

Kim, Y.M., Jae, J., Lee, H.W., Han, T.U., Lee, H., Park, S.H., Kim, S., Watanabe, C., Park, Y.K., 2016. Ex-situ catalytic pyrolysis of citrus fruit peels over mesoporous MFI and Al-MCM-41. Energy Convers. Manag. 125, 277–289. https://doi.org/10.1016/j.enconman.2016.02.065.

Koningen, J., Sjöström, K., 1998. Sulfur-deactivated steam reforming of gasified biomass. Ind. Eng. Chem. Res. 37, 341–346. https://doi.org/10.1021/ie970452t.

Kumagai, S., Yabuki, R., Kameda, T., Saito, Y., Yoshioka, T., 2020. Impact of Ni/Mg/Al catalyst composition on simultaneous H_2-rich syngas recovery and toxic HCN removal through a two-step polyurethane pyrolysis and steam reforming process. Ind. Eng. Chem. Res. 59, 9023–9033. https://doi.org/10.1021/acs.iecr.0c00931.

Kumagai, S., Hosaka, T., Kameda, T., Yoshioka, T., 2017. Removal of toxic HCN and recovery of H_2-rich syngas via catalytic reforming of product gas from gasification of polyimide over Ni/Mg/Al catalysts. J. Anal. Appl. Pyrolysis 123, 330–339. https://doi.org/10.1016/j.jaap.2016.11.012.

Kurniawan, T.A., Othman, M.H.D., Liang, X., Goh, H.H., Gikas, P., Chong, K., Chew, K.W., 2023. Challenges and opportunities for biochar to promote circular economy and carbon neutrality. J. Environ. Manag. 332, 117429 https://doi.org/10.1016/j.jenvman.2023.117429.

Lam, S.S., Liew, R.K., Cheng, C.K., Rasit, N., Ooi, C.K., Ma, N.L., Ng, J., Lam, W.H., Chong, C.T., Chase, H.A., 2018. Pyrolysis production of fruit peel biochar for potential use in treatment of palm oil mill effluent. J. Environ. Manag. 213, 400–408. https://doi.org/10.1016/j.jenvman.2018.02.092.

Landa, L., Remiro, A., Valecillos, J., Valle, B., Bilbao, J., Gayubo, A.G., 2022. Unveiling the deactivation by coke of $NiAl_2O_4$ spinel derived catalysts in the bio-oil steam reforming: role of individual oxygenates. Fuel 321, 124009. https://doi.org/10.1016/j.fuel.2022.124009.

Leppälahti, J., 1995. Formation of NH_3 and HCN in slow-heating-rate inert pyrolysis of peat, coal and bark. Fuel 74, 1363–1368. https://doi.org/10.1016/0016-2361(95)00091-I.

Li, J., Jia, P., Hu, X., Dong, D., Gao, G., Geng, D., Xiang, J., Wang, Y., Hu, S., 2018. Steam reforming of carboxylic acids for hydrogen generation: effects of aliphatic chain of the acids on their reaction behaviors. Mol. Catal. 450, 1–13. https://doi.org/10.1016/j.mcat.2018.02.027.

Lopez, G., Santamaria, L., Lemonidou, A., Zhang, S., Wu, C., Sipra, A.T., Gao, N., 2022. Hydrogen generation from biomass by pyrolysis. Nat. Rev. Methods Primers 2, 20. https://doi.org/10.1038/s43586-022-00097-8.

Miranda, R., Bustos-Martinez, D., Blanco, C.S., Villarreal, M.H.G., Cantú, M.E.R., 2009. Pyrolysis of sweet orange (Citrus sinensis) dry peel. J. Anal. Appl. Pyrolysis 86, 245–251. https://doi.org/10.1016/j.jaap.2009.06.001.

Mohan, D., Pittman Jr., C.U., Steele, P.H., 2006. Pyrolysis of wood/biomass for bio-oil: a critical review. Energy Fuels 20, 848–889. https://doi.org/10.1021/ef0502397.

Moogi, S., Lee, J., Jae, J., Sonne, C., Rinklebe, J., Heui Kim, D., Shiung Lam, S., Loke Show, P., Park, Y., 2021. Valorization of rice husk to aromatics via thermocatalytic conversion in the presence of decomposed methane. Chem. Eng. J. 417, 129264 https://doi.org/10.1016/j.cej.2021.129264.

Nahil, M.A., Wang, X., Wu, C., Yang, H., Chen, H., Williams, P.T., 2013. Novel bi-functional Ni-Mg-Al-CaO catalyst for catalytic gasification of biomass for hydrogen production with in situ CO_2 adsorption. RSC Adv. 3, 5583–5590. https://doi.org/10.1039/c3ra40576a.

Oasmaa, A., Solantausta, Y., Arpiainen, V., Kuoppala, E., Sipilä, K., 2010. Fast pyrolysis bio-oils from wood and agricultural residues. Energy Fuels 24, 1380–1388. https://doi.org/10.1021/ef901107f.

Ochoa, A., Aramburu, B., Valle, B., Resasco, D.E., Bilbao, J., Gayubo, A.G., Castaño, P., 2017. Role of oxygenates and effect of operating conditions in the deactivation of a Ni supported catalyst during the steam reforming of bio-oil. Green Chem. 19, 4315–4333. https://doi.org/10.1039/c7gc01432e.

Ong, K.L., Kaur, G., Pensupa, N., Uisan, K., Lin, C.S.K., 2018. Trends in food waste valorization for the production of chemicals, materials and fuels: case study South and Southeast Asia. Bioresour. Technol. 248, 100–112. https://doi.org/10.1016/j.biortech.2017.06.076.

Pan, C., Chen, A., Liu, Z., Chen, P., Lou, H., Zheng, X., 2012. Aqueous-phase reforming of the low-boiling fraction of rice husk pyrolyzed bio-oil in the presence of platinum catalyst for hydrogen production. Bioresour. Technol. 125, 335–339. https://doi.org/10.1016/j.biortech.2012.09.014.

Patsalou, M., Chrysargyris, A., Tzortzakis, N., Koutinas, M., 2020. A biorefinery for conversion of citrus peel waste into essential oils, pectin, fertilizer and succinic acid via different fermentation strategies. Waste Manage. (Tucson, Ariz.) 113, 469–477. https://doi.org/10.1016/j.wasman.2020.06.020.

Quispe, I., Navia, R., Kahhat, R., 2017. Energy potential from rice husk through direct combustion and fast pyrolysis: a review. Waste Manage. (Tucson, Ariz.) 59, 200–210. https://doi.org/10.1016/j.wasman.2016.10.001.

Remiro, A., Valle, B., Aguayo, A.T., Bilbao, J., Gayubo, A.G., 2013. Operating conditions for attenuating Ni/La_2O_3- αAl_2O_3 catalyst deactivation in the steam reforming of bio-oil aqueous fraction. Fuel Process. Technol. 115, 222–232. https://doi.org/10.1016/j.fuproc.2013.06.003.

Remón, J., Broust, F., Volle, G., García, L., Arauzo, J., 2015. Hydrogen production from pine and poplar bio-oils by catalytic steam reforming. Influence of the bio-oil composition on the process. Int. J. Hydrogen Energy 40, 5593–5608. https://doi.org/10.1016/j.ijhydene.2015.02.117.

Ren, J., Cao, J.P., Yang, F.L., Liu, Y.L., Tang, W., Zhao, X.Y., 2021. Understandings of catalyst deactivation and regeneration during biomass tar reforming: a crucial review. ACS Sustain. Chem. Eng. 9, 17186–17206. https://doi.org/10.1021/acssuschemeng.1c07483.

Santamaria, L., Lopez, G., Arregi, A., Amutio, M., Artetxe, M., Bilbao, J., Olazar, M., 2019. Stability of different Ni supported catalysts in the in-line steam reforming of biomass fast pyrolysis volatiles. Appl. Catal., B 242, 109–120. https://doi.org/10.1016/j.apcatb.2018.09.081.

Santamaria, L., Lopez, G., Fernandez, E., Cortazar, M., Arregi, A., Olazar, M., Bilbao, J., 2021. Progress on catalyst development for the steam reforming of biomass and waste plastics pyrolysis volatiles: a review. Energy Fuels 35 (21), 17051–17084. https://doi.org/10.1021/acs.energyfuels.1c01666.

Santamaria, L., Arregi, A., Lopez, G., Artetxe, M., Amutio, M., Bilbao, J., Olazar, M., 2020a. Effect of La_2O_3 promotion on a Ni/Al_2O_3 catalyst for H_2 production in the in-line biomass pyrolysis-reforming. Fuel 262, 116593. https://doi.org/10.1016/j.fuel.2019.116593.

Santamaria, L., Artetxe, M., Lopez, G., Cortazar, M., Amutio, M., Bilbao, J., Olazar, M., 2020b. Effect of CeO_2 and MgO promoters on the performance of a Ni/Al_2O_3 catalyst in the steam reforming of biomass pyrolysis volatiles. Fuel Process. Technol. 198, 106223 https://doi.org/10.1016/j.fuproc.2019.106223.

Santiago, B., Moreira, M.T., Feijoo, G., González-García, S., 2020. Identification of environmental aspects of citrus waste valorization into D-limonene from a biorefinery approach. Biomass Bioenergy 143, 105844. https://doi.org/10.1016/j.biombioe.2020.105844.

Sharma, R.K., Wooten, J.B., Baliga, V.L., Hajaligol, M.R., 2001. Characterization of chars from biomass-derived materials: pectin chars. Fuel 80, 1825–1836. https://doi.org/10.1016/S0016-2361(01)00066-7.

Stone, J., Garcia-Garcia, G., Rahimifard, S., 2019. Development of a pragmatic framework to help food and drink manufacturers select the most sustainable food waste valorisation strategy. J. Environ. Manag. 247, 425–438. https://doi.org/10.1016/j.jenvman.2019.06.037.

Teigiserova, D.A., Tiruta-Barna, L., Ahmadi, A., Hamelin, L., Thomsen, M., 2021. A step closer to circular bioeconomy for citrus peel waste: a review of yields and technologies for sustainable management of essential oils. J. Environ. Manag. 280, 111832 https://doi.org/10.1016/j.jenvman.2020.111832.

Tian, B., Xu, L., Jing, M., Liu, N., Tian, Y., 2021. A comprehensive evaluation on pyrolysis behavior, kinetics, and primary volatile formation pathways of rice husk for application to catalytic valorization. Fuel Process. Technol. 214, 106715 https://doi.org/10.1016/j.fuproc.2020.106715.

Torres, W., Pansare, S.S., Goodwin, J.G., 2007. Hot gas removal of tars, ammonia, and hydrogen sulfide from biomass gasification gas. Catal. Rev. Sci. Eng. 49, 407–456. https://doi.org/10.1080/01614940701375134.

Trane-Restrup, R., Jensen, A.D., 2015. Steam reforming of cyclic model compounds of bio-oil over Ni-based catalysts: product distribution and carbon formation. Appl. Catal., B 165, 117–127. https://doi.org/10.1016/j.apcatb.2014.09.026.

Vargas, G., Zapata, B., Valenzuela, M.A., Alfaro, S., 2015. Orange peel oxidative gasification on Ni catalysts promoted with CaO, CeO_2 or K_2O. J. Nanosci. Nanotechnol. 15, 6663–6668. https://doi.org/10.1166/jnn.2015.10876.

Vicente, J., Montero, C., Ereña, J., Azkoiti, M.J., Bilbao, J., Gayubo, A.G., 2014. Coke deactivation of Ni and Co catalysts in ethanol steam reforming at mild temperatures in a fluidized bed reactor. Int. J. Hydrogen Energy 39, 12586–12596. https://doi.org/10.1016/j.ijhydene.2014.06.093.

Waheed, Q.M.K., Wu, C., Williams, P.T., 2016. Pyrolysis/reforming of rice husks with a Ni–dolomite catalyst: influence of process conditions on syngas and hydrogen yield. J. Energy Inst. 89, 657–667. https://doi.org/10.1016/j.joei.2015.05.006.

Wang, Y., Hu, X., Song, Y., Min, Z., Mourant, D., Li, T., Gunawan, R., Li, C.Z., 2013. Catalytic steam reforming of cellulose-derived compounds using a char-supported iron catalyst. Fuel Process. Technol. 116, 234–240. https://doi.org/10.1016/j.fuproc.2013.07.014.

Windeatt, J.H., Ross, A.B., Williams, P.T., Forster, P.M., Nahil, M.A., Singh, S., 2014. Characteristics of biochars from crop residues: potential for carbon sequestration and soil amendment. J. Environ. Manag. 146, 189–197. https://doi.org/10.1016/j.jenvman.2014.08.003.

Xiao, X., Cao, J., Meng, X., Le, D.D., Li, L., Ogawa, Y., Sato, K., Takarada, T., 2013. Synthesis gas production from catalytic gasification of waste biomass using nickel-loaded brown coal char. Fuel 103, 135–140. https://doi.org/10.1016/j.fuel.2011.06.077.

Xiao, X., Meng, X., Le, D.D., Takarada, T., 2011. Two-stage steam gasification of waste biomass in fluidized bed at low temperature: parametric investigations and performance optimization. Bioresour. Technol. 102, 1975–1981. https://doi.org/10.1016/j.biortech.2010.09.016.

Yang, H., Yan, R., Chen, H., Lee, D.H., Zheng, C., 2007. Characteristics of hemicellulose, cellulose and lignin pyrolysis. Fuel 86, 1781–1788. https://doi.org/10.1016/j.fuel.2006.12.013.

Yin, W., Guilhaume, N., Schuurman, Y., 2020. Model biogas reforming over Ni-Rh/$MgAl_2O_4$ catalyst. Effect of gas impurities. Chem. Eng. J. 398, 125534 https://doi.org/10.1016/j.cej.2020.125534.

Zema, D.A., Calabrò, P.S., Folino, A., Tamburino, V., Zappia, G., Zimbone, S.M., 2018. Valorisation of citrus processing waste: a review. Waste Manage. (Tucson, Ariz.) 80, 252–273. https://doi.org/10.1016/j.wasman.2018.09.024.

Zhou, S., Xu, Y., Wang, C., Tian, Z., 2011. Pyrolysis behavior of pectin under the conditions that simulate cigarette smoking. J. Anal. Appl. Pyrolysis 91, 232–240. https://doi.org/10.1016/j.jaap.2011.02.015.